Mice lacking the inhibitory collagen receptor LAIR-1 exhibit a mild thrombocytosis and hyperactive platelets

Smith, Christopher; Thomas, Steven; RASLAN, Zaher; Patel, Pushpa; Byrne, Maxwell; Lordkipanidze, Marie; Bem, Danai; Meyaard, Linde; Senis, Yotis; Watson, Steve; Mazharian, Alexandra

DOI:
10.1161/ATVBAHA.117.309253

Document Version
Peer reviewed version

Citation for published version (Harvard):
Smith, C, Thomas, S, RASLAN, Z, Patel, P, Byrne, M, Lordkipanidze, M, Bem, D, Meyaard, L, Senis, Y, Watson, S & Mazharian, A 2017, 'Mice lacking the inhibitory collagen receptor LAIR-1 exhibit a mild thrombocytosis and hyperactive platelets', *Arteriosclerosis Thrombosis and Vascular Biology*, vol. 37, no. 5, pp. 823-835. https://doi.org/10.1161/ATVBAHA.117.309253

Mice lacking the inhibitory collagen receptor LAIR-1 exhibit a mild thrombocytosis and hyperactive platelets

Christopher W. Smith[1], Steven G. Thomas[1], Zaher Raslan[1], Pushpa Patel[1], Maxwell Byrne[1], Marie Lordkipanidzé[1], Danai Bem[2], Linde Meyaard[3], Yotis A. Senis[1], Steve P. Watson[1] and Alexandra Mazharian[1]

[1]Institute of Cardiovascular Sciences, College of Medical and Dental Sciences, University of Birmingham, Birmingham, B15 2TT, United Kingdom. [2]Institute of Applied Health Research, College of Medical and Dental Sciences, University of Birmingham, Birmingham, B15 2TT, United Kingdom. [3]Laboratory of Translational Immunology, Department of Immunology, University Medical Center Utrecht, Utrecht, The Netherlands

AM is a BHF Intermediate Basic Science Research Fellow (FS/15/58/31784). YAS is a BHF Senior Basic Science Research Fellow (FS/13/1/29894). SPW holds a BHF Chair (CH/03/003). This work was supported by the BHF project grant held by AM (PG/13/51/30296).

Corresponding author: Alexandra Mazharian, Institute of Cardiovascular Sciences, College of Medical and Dental Sciences, University of Birmingham, Birmingham, B15 2TT, UK; tel: +44-(0)121-415-8678; email: a.mazharian@bham.ac.uk

Text word count: 5515
Abstract word count: 235
Number of figures: 7
Number of references: 29
Number of Supplemental figures: 9

Abstract

Objective: Leukocyte-associated immunoglobulin-like receptor-1 (LAIR-1) is a collagen receptor that belongs to the inhibitory immunoreceptor tyrosine-based inhibition motif (ITIM)-containing receptor family. It is an inhibitor of signalling via the immunoreceptor tyrosine-based activation motif (ITAM)-containing collagen receptor complex, GPVI-FcRγ-chain. It is expressed on hematopoietic cells, including immature megakaryocytes, but is not detectable on platelets. Although the inhibitory function of LAIR-1 has been described in leukocytes, its physiological role in megakaryocytes and in particular in platelet formation has not been explored. In this study, we investigate the role of LAIR-1 in megakaryocyte development and platelet production by generating LAIR-1-deficient mice.

Approach and Results: Mice lacking LAIR-1 exhibit a significant increase in platelet counts, a prolonged platelet half-life *in vivo* and increased proplatelet formation *in vitro*. Interestingly, platelets from LAIR-1-deficient mice exhibit an enhanced reactivity to collagen and the GPVI-specific agonist collagen-related peptide (CRP) despite not expressing LAIR-1, and mice showed enhanced thrombus formation in the carotid artery following ferric chloride injury. Targeted deletion of LAIR-1 in mice results in an increase in signalling downstream of the GPVI-FcRγ-chain and integrin αIIbβ3 in megakaryocytes due to enhanced Src family kinase (SFK) activity.

Conclusions: Findings from this study demonstrate that ablation of LAIR-1 in megakaryocytes leads to increased SFK activity and downstream signalling in response to collagen that is transmitted to platelets, rendering them hyper-reactive specifically to agonists that signal through Syk tyrosine kinases, but not to G protein-coupled receptors.

Key words: LAIR-1, ITIM, SFK, megakaryopoiesis, thrombocytosis, platelet hyperactivity

Running title: hyperactive platelets in LAIR-1 KO mice

Nonstandard Abbreviations and Acronyms
CRP: collagen-related peptide
Erk1/2: extracellular signal-regulated kinase
SFK: Src family kinase
Tpo: thrombopoietin
WT: wild-type

Introduction

For an adequate function of platelets and megakaryocytes, a tight balance between stimulatory and inhibitory signals is required. Inhibitory receptors that carry immunoreceptor tyrosine-based inhibition motifs (ITIMs) in their cytoplasmic tail play an essential role in the regulation of megakaryocyte and platelet reactivity[1,2]. Platelets express at least five ITIM-containing receptors, PECAM-1, CEACAM-1, CEACAM-2, TLT-1 and G6b-B. Platelet endothelial cell adhesion molecule-1 **(**PECAM-1) is a well characterised ITIM-containing receptor that has been reported to inhibit signaling via the immunocreceptor tyrosine-based activation motif (ITAM)-containing collagen receptor complex GPVI-FcR γ-chain and thrombin-mediated platelet activation[1]. Carcinoembryonic antigen-related cell adhesion molecule (CEACAM)-1 was shown to have a similar function in platelets to that of PECAM-1[3]. CEACAM-2 is a novel platelet immunoreceptor that has been shown to act as a negative regulator of platelet GPVI-FcR γ-chain and of the hemi-immunoreceptor tyrosine-based activation motif (hemi-ITAM)-containing podoplanin receptor CLEC-2 pathways[4]. In contrast, the platelet-specific ITIM-containing triggering receptor expressed in myeloid cells-like transcript-1 (TLT-1) is up-regulated on the surface of activated platelets and plays a role in supporting, rather than inhibiting, platelet activation[5]. Unique among ITIM-containing receptors, G6b-B is highly abundant in mature megakaryocytes and platelets and is constitutively phosphorylated and associated with the SH2 domain-containing non-transmembrane protein-tyrosine phosphatases (PTPs) Shp1 and Shp2[6]. We recently reported that G6b-B is a major regulator of megakaryocyte/platelet homeostasis and platelet reactivity[2,7].

Leukocyte-associated immunoglobulin (Ig)-like receptor-1 (LAIR-1), also known as CD305, is a collagen receptor that belongs to the inhibitory Ig-ITIM family[8]. LAIR-1 is widely expressed on hematopoietic cells, including immature megakaryocytes, but is not detectable in platelets[9]. LAIR-1 possesses a single extracellular Ig variable domain and 2 ITIMs in its cytoplasmic tail that mediate its inhibitory capacity through the interaction with Shp1, Shp2 and C-terminal Src kinase (Csk)[10,11]. LAIR-1 binds with higher affinity than GPVI to glycine-proline-hydroxyproline (GPO) repeat motifs in collagen[12,13].

Previously, we have shown that co-expression of LAIR-1 with GPVI in transiently transfected DT40 chicken B cells mediates strong inhibition of collagen-mediated activation of a NFAT reporter assay[14]. Several studies have shown that LAIR-1 also functions as an inhibitory receptor on immune cells and is involved in the regulation of hematopoietic cell differentiation[15-18]. In addition, recent studies report that LAIR-1 is essential for acute myeloid leukaemia development[19,20]. However, the role of LAIR-1 in megakaryocyte development and platelet formation is not known.

In this study, we investigate the role of LAIR-1 in megakaryopoiesis and platelet activation. We show that mice lacking LAIR-1 exhibit a mild thrombocytosis, increased proplatelet formation *in vitro* and produce hyperactive platelets. Furthermore, LAIR-1-deficient megakaryocytes exhibit increased reactivity to collagen and increased αIIbβ3 outside-in signalling despite having normal cell surface levels of the collagen receptors GPVI and the integrin α2β1, and of the fibrinogen integrin αIIbβ3. The increase in reactivity observed in LAIR-1-deficient megakaryocytes is also seen in platelets, suggesting transfer of activation signals from megakaryocytes to platelets.

Materials and Methods

Materials and Methods are available in the online-only Data Supplement.

Results

LAIR-1 and GPVI are inversely expressed during megakaryopoiesis *in vitro*

We first analysed the expression of LAIR-1 alongside other major surface glycoproteins during mouse megakaryocyte differentiation by flow cytometry. Bone marrow progenitor cells were isolated from wild-type (WT) mice and cultured in the presence of 20 ng/ml Tpo for 8 days. Cells were harvested every day and receptor surface expression measured by flow cytometry. LAIR-1 was highly expressed on mouse hematopoietic stem cells and its expression decreased during megakaryopoiesis **(Figure 1A-B)**, whereas the opposing relationship was observed for the collagen receptors, GPVI and $\alpha 2\beta 1$. Importantly, GPVI and $\alpha 2\beta 1$ were highly expressed on mouse platelets, but LAIR-1 expression was not detectable by flow cytometry or western blot **(Figure 1B and Figure 2Ai)**. These results demonstrate that GPVI and LAIR-1 are inversely expressed during mouse megakaryopoiesis *in vitro* as is the case for human megakaryocytes[9]. However, a subset of intermediate megakaryocytes expressed both activatory and inhibitory receptors for collagen. In this population of megakaryocytes, the GPVI-specific agonist convulxin, which does not bind to LAIR-1[14], stimulated phosphorylation of LAIR-1 **(Figure 1C)**.

LAIR-1-deficient mice exhibit mild thrombocytosis and increased platelet half-life

To study the physiological function of LAIR-1, we generated LAIR-1-deficient mice **(Supplemental Figure I)**. Homozygous LAIR-1 knockout mice (LAIR-1 KO) were born at Mendelian frequencies, were fertile, and survived for >25 weeks with no overt growth or developmental defects. By western blotting, LAIR-1 was not detectable in immature megakaryocytes from LAIR-1 KO mice, nor in platelets from WT and LAIR-1 KO mice **(Figure 2Ai)**. Haematological analysis revealed that LAIR-1 KO mice displayed a mild thrombocytosis (25% increase in platelet count) with unchanged platelet volume **(Figure 2Aii-iii)**. Platelets and megakaryocytes from LAIR-1 KO mice have normal organelles and granule content as assessed by transmission electron microscopy (**Figure 2B** and not shown). LAIR-1 KO mice did not exhibit a bleeding diathesis following tail injury **(Supplemental Figure II)**. In addition, megakaryocyte counts were normal in the spleen and bone marrow of LAIR-1 KO mice **(Supplemental Figure IIIA,C)** and reticulin staining revealed no evidence of tissue damage in the spleen and bone marrow of LAIR-1 KO mice **(Supplemental Figure IIIB)**. To investigate whether the thrombocytosis was the result of decreased platelet clearance, platelet half-life was measured *in vivo*. Interestingly, we found that the half-life of platelets from LAIR-1 KO mice was increased by 17% **(Figure 2C)**, thereby accounting for the mild thrombocytosis.

Normal megakaryocyte development, but increased proplatelet formation in LAIR-1 KO mice

We next investigated whether LAIR-1 regulates megakaryocyte differentiation *in vitro* by analysing their DNA content during development. The absence of LAIR-1 had no effect on megakaryocyte development as shown by a normal ploidy pattern **(Figure 3Ai-ii)** and cellular appearance (data not shown). LAIR-1-deficient megakaryocytes

exhibited a marked increase in spreading on a fibrinogen-coated surface **(Figure 3Bi-ii)**, despite having normal levels of αIIbβ3 **(Table 1)**, suggesting increased outside-in integrin signalling. In addition, the percentage of LAIR-1-deficient megakaryocytes forming proplatelets was elevated and an increased branching of proplatelets was also observed **(Figure 3Ci-iii)**. These results demonstrate that LAIR-1 exhibits a tonic inhibitory effect on megakaryocyte spreading on fibrinogen and on platelet formation. Since LAIR-1 is a collagen receptor, we have also investigated megakaryocyte spreading and proplatelet formation on collagen. We show that LAIR-1-deficient megakaryocytes spread normally on collagen, and that neither WT nor LAIR-1 KO megakaryocytes formed proplatelets on collagen **(Supplemental Figure IV** and data not shown**)**.

Unchanged thrombopoietin signalling, but increased reactivity to collagen in LAIR-1-deficient megakaryocytes

Having demonstrated increased spreading and proplatelet formation in LAIR-1 KO megakaryocytes, we investigated the molecular basis of these defects. We focused on Tpo- and integrin-mediated Erk1/2 phosphorylation and SFK activation, as we have previously demonstrated that Erk1/2 plays a critical role in primary megakaryocyte differentiation, motility, and proplatelet formation[21], and that SFKs regulate megakaryocyte differentiation and platelet production[21]. Phospho-specific antibodies were used to monitor Erk1/2 and SFK activation. Tpo-mediated Erk1/2 activation was normal in LAIR-1-deficient megakaryocytes **(Figure 4Ai)**, consistent with the normal growth and ploidy of these cells **(Figure 3Ai-ii)**. SFK activation, which lies upstream of Erk1/2, was, however enhanced in resting LAIR-1-deficient megakaryocytes compared to controls **(Figure 4Aii)**, suggesting that basal SFK activity was increased. Despite the extent of basal SFK activation being increased, SFKs were phosphorylated to the same extent on their activation loop (Tyr-418) by Tpo in control and mutant megakaryocytes **(Figure 4Aii)**. In addition, basal and integrin αIIbβ3-mediated Erk1/2 and SFK activation were increased in fibrinogen-adhered LAIR-1-deficient megakaryocytes **(Figure 4Bi-ii)**, consistent with the increased megakaryocyte spreading and proplatelet formation **(Figure 3Bi-ii and Figure 3Ci-iii)**.

Since LAIR-1 is an inhibitory collagen receptor, we investigated GPVI signalling in LAIR-1-deficient megakaryocytes. Interestingly, we show that phosphorylation of SFK Tyr-418, the tyrosine kinase Syk on its activation loops (Syk Tyr-519/520) and of its downstream target PLCγ2 on Tyr-1217, all of which are indicators of activation, were significantly increased in LAIR-1-deficient resting and convulxin-stimulated megakaryocytes **(Figure 4Ci-iii)**, despite having a normal surface level of GPVI **(Table 1)**. However, phosphorylation of Src, Fyn and Lyn at their C-terminal inhibitory tyrosine residues, Tyr-529, Tyr-530 and Tyr-507 respectively were unchanged **(Supplemental Figure V)**.

LAIR-1-deficient mice exhibit increased platelet function

Platelet aggregation and ATP secretion were measured to investigate whether the absence of LAIR-1 in megakaryocytes alters platelet function. An increase in response to collagen, which binds to GPVI and α2β1, and to the GPVI-specific agonist CRP, but not to convulxin, was observed in platelets from LAIR-1 KO mice using light transmission aggregometry **(Figure 5Ai-iii, Figure 5Bi-iii and Supplemental Figure VIAi-ii respectively)**, despite having normal expression

levels of the collagen receptors GPVI and α2β1 **(Table 2)**. The expression levels of integrin αIIbβ3, GPIbα and of the ITIM-containing receptors G6b-B and PECAM-1 remained unchanged **(Table 2)**. Platelet aggregation in response to thrombin, U46619 and ADP were normal in LAIR-1 KO mice compared with WT controls **(Figure 5Ci-iii and Supplemental Figure VIBi-iii)**. Similar results were observed using a 96-well plate aggregation assay **(Supplemental Figure VIC)**, which confirmed greater sensitivity of platelets from LAIR-1 KO mice to collagen-induced aggregation. Consistent with this observation, P-selectin exposure, fibrinogen binding and integrin activation were also increased in response to CRP, but not to thrombin in LAIR-1 KO mice **(Figure 5D and Supplemental Figure VID)**.

We next investigated platelet spreading on a fibrinogen-coated surface as this is an important aspect of platelet function that is dependent on the integrin αIIbβ3 for adhesion and cytoskeletal remodelling[22]. Platelets from LAIR-1 KO mice exhibited an increase in spreading on fibrinogen in comparison to WT platelets **(Figure 6Ai-ii)**, suggesting that LAIR-1 negatively regulates this process. However, when pre-activated with 0.1 U/mL thrombin, platelets from LAIR-1 KO mice spread normally **(Figure 6Ai-ii)**. Therefore, LAIR-1 is involved in the regulation of αIIbβ3 outside-in signalling, but not the regulation of protease-activated receptor-4 (PAR-4) signalling. Whole cell lysates prepared from fibrinogen-spread and non-adherent platelets exhibited an increase in phosphorylation of Src Tyr-418 and Syk Tyr-519/520, in platelets from LAIR-1 KO mice **(Figure 6Bi-ii)**, consistent with the increase in spreading, whereas phosphorylation of Src Tyr-529, Fyn Tyr-530 and Lyn Tyr-507 were unchanged **(Supplemental Figure VII)**, providing further evidence of a proximal signalling defect. Integrin αIIbβ3 outside-in signalling also regulates clot retraction. To study whether the loss of LAIR-1 alters clot retraction, clot formation was induced in PRP by addition of a high concentration of thrombin (10 U/mL) in the presence of 2 mM Ca^{2+} and was monitored over time. No differences were observed and the excess fluid extruded after clot retraction was similar in WT and LAIR-1 KO mice **(Supplemental Figure VIII)**.

Increased GPVI-mediated signalling in platelets from LAIR-deficient mice

The molecular basis of the increase in reactivity to collagen and CRP was investigated by monitoring protein phosphorylation. Western blotting revealed a general increase in tyrosine phosphorylation in response to CRP in platelets from LAIR-1KO mice **(Figure 7Ai)**, including FcR γ-chain and SFK Tyr-418 **(Figure 7Aii)**. Further investigation revealed increased phosphorylation Syk Tyr-519/520 and increased phosphorylation of its downstream target PLCγ2 Tyr-1217 **(Figure 7Bi-ii)**, whereas phosphorylation of Src Tyr-529, Fyn Tyr-530 and Lyn Tyr-507 were unchanged **(Supplemental Figure IXAi-ii)**. This demonstrated that deletion of LAIR-1 in megakaryocytes results in increased SFK activity and downstream GPVI signalling. Platelets from LAIR-1 KO mice spread normally on collagen *in vitro* as shown by normal surface area coverage **(Supplemental Figure IXBi-ii)**. However, interestingly they formed larger aggregates on a collagen matrix under arterial shear, and covered a larger surface area **(Figure 7C)**. The physiological role of LAIR-1 in arterial thrombosis was also investigated *in vivo* using two distinct assays, namely the laser- and ferric chloride-induced injury models. We found that, in the laser injury model in cremaster arterioles, thrombus formation was unaffected in LAIR-1 KO mice **(Figure 7Di-ii and Supplemental Videos SI and SII)**. However, using the ferric chloride injury model in the carotid artery, we show that the rate and extent of

thrombus formation is significantly increased in the LAIR-1 KO mice compared with litter-matched WT mice **(Figure 7Ei-iii and Supplemental Videos SIII and SIV).** These findings correlate with the increase in platelet reactivity to collagen demonstrated in *vitro*.

Taken together, these findings demonstrate that the lack of inhibition of ITAM signalling in LAIR-1-deficient megakaryocytes is transferred to platelets, resulting in enhanced GPVI-mediated signalling through increased SFK activity resulting in greater platelet activation and a predisposition to thrombosis that is dependent on the type of injury and vasculature.

Discussion

In this study, we investigated the role of LAIR-1 in megakaryocyte development and platelet production by generating and characterising LAIR-1 KO mice. We demonstrate for the first time that LAIR-1 is a negative regulator of platelet production and reactivity to collagen and fibrinogen. Mice lacking LAIR-1 exhibit a 25% increase in platelet counts, a prolonged platelet half-life *in vivo* and increased proplatelet formation *in vitro*. Interestingly, platelets from LAIR-1 KO mice exhibit an enhancement of reactivity to GPVI and αIIbβ3 agonists, despite not expressing LAIR-1 and having normal receptor levels, and formed larger aggregates on a collagen matrix under arterial shear. As a consequence, LAIR-1 KO mice exhibited increased thrombus formation following ferric chloride-induced carotid artery injury, which has been shown to be GPVI-dependent[23], but not following laser-induced injury of cremaster arterioles, which is tissue factor and thrombin-dependent[23]. In addition, the composition of the vessel wall and rheological characteristics differ between these models, which likely influences the differences observed. Findings from this study demonstrate that ablation of LAIR-1 in megakaryocytes leads to an increased SFK activity and downstream signalling in response to collagen that is transmitted to platelets, rendering them hyper-reactive specifically to agonists that signal through SFKs, but not through G protein-coupled receptors.

We first examined the expression of collagen receptors (LAIR-1, GPVI, α2β1) and surface-marker expression of CD34, GPIbα and αIIbβ3 at different stages of megakaryocyte maturation. During murine megakaryocyte maturation, the inhibitory collagen receptor LAIR-1 is downregulated while the activating collagen receptor GPVI is upregulated. However, a subset of cells co-express these collagen receptors with opposite functions, as previously shown during human megakaryopoiesis[9]. These findings raise the question of why LAIR-1 would be expressed at these early stages of megakaryocyte differentiation. One possible explanation is that this could prevent the excessive activation of immature megakaryocytes exposed to surrounding collagens. The main collagen receptors expressed by megakaryocytes are the high affinity integrin α2β1, the low affinity ITAM-containing receptor GPVI-FcRγ-chain complex, and LAIR-1, which has the same binding site as GPVI, but with a considerably higher affinity[12].

Deletion of LAIR-1 in mice leads to an increase in the number of circulating platelets compared to litter-matched controls. Despite this, megakaryocyte counts were normal in the spleen and bone marrow of LAIR-1 KO mice and reticulin staining revealed no evidence of tissue damage in the spleen and bone marrow of LAIR-1 KO mice. We show that platelet half-life is increased thereby accounting for the mild thrombocythemia. Recent studies have highlighted the role of glycan modification on platelet surface proteins mediating platelet clearance[24,25]. Indeed, lifespan of

circulating platelets is determined by sialic acid loss that triggers platelet removal by the hepatic Ashwell-Morell receptor (AMR)[25]. Circulating platelets become desialylated as they age, however, in preliminary studies, we did not observe a change in staining for sialic acid in platelets from LAIR-1 KO mice. Platelet survival also depends on the interplay between pro-survival and pro-apopotic signals[26] and a change in either of these could underlie the increase in platelet life-span.

We also found that LAIR-1 KO mice exhibit normal megakaryocyte development as measured by ploidy levels but enhanced proplatelet formation on fibrinogen suggesting that platelet biogenesis is enhanced, providing a further basis for the increase in platelet count. We investigated the molecular mechanism underlying the increased proplatelet formation exhibited by the LAIR-1-deficient megakaryocytes by examining phosphorylation of key signalling proteins downstream of integrin αIIbβ3. We found that Erk1/2 and SFK activation were increased in fibrinogen adherent LAIR-1-deficient megakaryocytes as is similarly the case in platelets, which also exhibit increased GPVI signalling. This raises the possibility that a change in SFK activity in megakaryocytes could potentially underlie both the increase in platelet production and reactivity to GPVI and integrin αIIbβ3 agonists observed in platelets. Despite the increase in SFK activity, megakaryocytes and platelets from LAIR-1 KO mice spread normally on collagen. We suspect this is due to the moderate phenotype and synergistic effects of multiple receptors and feedback pathways involved, masking any defect.

Previous work by Meyaard et al demonstrated that LAIR-1 mediates its inhibitory effect through its interaction with Shp1 and Shp2[10]. LAIR-1 has also been shown to recruit Csk to the plasma membrane[10], which inhibits SFK activity by phosphorylating the C-terminal inhibitory tyrosine residue. Here, we report that LAIR-1 KO megakaryocytes exhibit increased basal SFK activity that is then transferred to platelets, rendering them hyper-responsive to collagen and fibrinogen, and represents a new paradigm of how platelet reactivity can be modulated. Although the mechanism underlying the increase in SFK activity in LAIR-1 KO megakaryocytes remains undefined, we hypothesize it is due to decreased compartmentalization of Shp1, Shp2 or Csk at the plasma membrane, all of which have been implicated in regulating SFK activity either directly by modulating the relative level of phosphorylation of the C-terminal inhibitory and activation loop tyrosine residues, or indirectly through regulation of adaptor proteins that unclamp and activate SFKs[27]. It should be noted that phosphorylation of the C-terminal inhibitory tyrosine residue of SFKs does not always correlate with SFK activity, whereas phosphorylation of the activation loop does[28]. Further work is needed to elucidate the exact mechanism underlying the increase in SFK activity in LAIR-1 KO megakaryocytes, and why it remains elevated in resting platelets.

The present study adds to the growing evidence that ITIM-containing receptors are critical regulators of platelet formation and function and sheds new light on the role of the collagen receptor LAIR-1 in regulating the basal activating state of megakaryocytes. LAIR-1 is therefore the third ITIM receptor that has been shown to regulate platelet formation. Mice deficient in PECAM-1 exhibit a significant decrease in platelet recovery following immune thrombocytopenia and increased platelet reactivity to collagen[29]. In contrast, mice lacking G6b-B have a pronounced thrombocytopenia and increased GPVI shedding[2]

This study establishes that deletion of LAIR-1 in megakaryocytes disrupts the homeostatic balance of megakaryocytes and platelets, shifting the balance to a

prothrombotic state due to concomitant increases in platelet count and reactivity. Moreover, this study demonstrates that changes in the activation state of signalling proteins within the megakaryocytes leads to changes in platelets that are released into the circulation. Alteration in the megakaryocyte signalling proteins can therefore influence platelet functional responses. While substantial progress has been made in understanding the mechanisms that regulate thrombopoiesis and platelet formation, we have yet to fully uncover what signalling pathways initiate and regulate these processes. A better understanding of these processes may result in therapies that stimulate immediate platelet production from existing megakaryocytes.

Acknowledgements
The authors thank the members of the Biomedical Service Unit for their technical support. We would like to thank Dr. Jun Mori for her expertise with the laser injury model and Professor Alastair Poole and Dr. Christopher M. Williams (University of Bristol) for their expertise with the ferric chloride injury model. A.M. designed and performed experiments, collected, analysed and interpreted data, contributed intellectually, wrote and revised the manuscript. C.S., S.G.T., Z.R., M.L., M.B. and D.B. performed experiments, analysed, interpreted data and revised the manuscript. P.P. maintained the LAIR-1 mouse colonies and assisted with the experiments. L.M. revised the manuscript. Y.A.S. and S.P.W. designed experiments, interpreted data, contributed intellectually and revised the manuscript.

Source of funding
This work was supported by the British Heart Foundation (BHF) project grant PG/13/51/30296. A.M. is a BHF Intermediate Basic Science Research Fellow and principal investigator of this study (FS/15/58/31784). Y.A.S. is a BHF Senior Basic Science Research Fellow (FS/13/1/29894). S.P.W. is a BHF Chair (CH/03/003).

Disclosure
None

References
1. Falati S, Patil S, Gross PL, Stapleton M, Merrill-Skoloff G, Barrett NE, Pixton KL, Weiler H, Cooley B, Newman DK, Newman PJ, Furie BC, Furie B, Gibbins JM. Platelet PECAM-1 inhibits thrombus formation in vivo. *Blood*. 2006;107:535-541.
2. Mazharian A, Wang YJ, Mori J, Bem D, Finney B, Heising S, Gissen P, White JG, Berndt MC, Gardiner EE, Nieswandt B, Douglas MR, Campbell RD, Watson SP, Senis YA. Mice lacking the ITIM-containing receptor G6b-B exhibit macrothrombocytopenia and aberrant platelet function. *Sci Signal*. 2012;5:ra78.
3. Wong C, Liu Y, Yip J, Chand R, Wee JL, Oates L, Nieswandt B, Reheman A, Ni H, Beauchemin N, Jackson DE. CEACAM1 negatively regulates platelet-collagen interactions and thrombus growth in vitro and in vivo. *Blood*. 2009;113:1818-1828.
4. Alshahrani MM, Yang E, Yip J, Ghanem SS, Abdallah SL, deAngelis AM, O'Malley CJ, Moheimani F, Najjar SM, Jackson DE. CEACAM2 negatively regulates hemi (ITAM-bearing) GPVI and CLEC-2 pathways and thrombus growth in vitro and in vivo. *Blood*. 2014;124:2431-2441.
5. Washington AV, Gibot S, Acevedo I, et al. TREM-like transcript-1 protects against inflammation-associated hemorrhage by facilitating platelet aggregation in mice and humans. *J Clin Invest*. 2009;119:1489-1501.

6. Senis YA, Tomlinson MG, Garcia A, et al. A comprehensive proteomics and genomics analysis reveals novel transmembrane proteins in human platelets and mouse megakaryocytes including G6b-B, a novel immunoreceptor tyrosine-based inhibitory motif protein. *Mol Cell Proteomics*. 2007;6:548-564.
7. Mazharian A, Mori J, Wang YJ, Heising S, Neel BG, Watson SP, Senis YA. Megakaryocyte-specific deletion of the protein-tyrosine phosphatases Shp1 and Shp2 causes abnormal megakaryocyte development, platelet production, and function. *Blood*. 2013;121:4205-4220.
8. Meyaard L. The inhibitory collagen receptor LAIR-1 (CD305). *J Leukoc Biol*. 2008;83:799-803.
9. Steevels TA, Westerlaken GH, Tijssen MR, Coffer PJ, Lenting PJ, Akkerman JW, Meyaard L. Co-expression of the collagen receptors leukocyte-associated immunoglobulin-like receptor-1 and glycoprotein VI on a subset of megakaryoblasts. *Haematologica*. 2010;95:2005-2012.
10. Verbrugge A, Rijkers ES, de Ruiter T, Meyaard L. Leukocyte-associated Ig-like receptor-1 has SH2 domain-containing phosphatase-independent function and recruits C-terminal Src kinase. *Eur J Immunol*. 2006;36:190-198.
11. Verbrugge A, Ruiter Td T, Clevers H, Meyaard L. Differential contribution of the immunoreceptor tyrosine-based inhibitory motifs of human leukocyte-associated Ig-like receptor-1 to inhibitory function and phosphatase recruitment. *Int Immunol*. 2003;15:1349-1358.
12. Lebbink RJ, de Ruiter T, Adelmeijer J, Brenkman AB, van Helvoort JM, Koch M, Farndale RW, Lisman T, Sonnenberg A, Lenting PJ, Meyaard L. Collagens are functional, high affinity ligands for the inhibitory immune receptor LAIR-1. *J Exp Med*. 2006;203:1419-1425.
13. Brondijk TH, de Ruiter T, Ballering J, Wienk H, Lebbink RJ, van Ingen H, Boelens R, Farndale RW, Meyaard L, Huizinga EG. Crystal structure and collagen-binding site of immune inhibitory receptor LAIR-1: unexpected implications for collagen binding by platelet receptor GPVI. *Blood*. 2010;115:1364-1373.
14. Tomlinson MG, Calaminus SD, Berlanga O, Auger JM, Bori-Sanz T, Meyaard L, Watson SP. Collagen promotes sustained glycoprotein VI signaling in platelets and cell lines. *J Thromb Haemost*. 2007;5:2274-2283.
15. Meyaard L. LAIR and collagens in immune regulation. *Immunol Lett*. 2010;128:26-28.
16. Tang X, Tian L, Esteso G, Choi SC, Barrow AD, Colonna M, Borrego F, Coligan JE. Leukocyte-associated Ig-like receptor-1-deficient mice have an altered immune cell phenotype. *J Immunol*. 2012;188:548-558.
17. Xue J, Zhang X, Zhao H, Fu Q, Cao Y, Wang Y, Feng X, Fu A. Leukocyte-associated immunoglobulin-like receptor-1 is expressed on human megakaryocytes and negatively regulates the maturation of primary megakaryocytic progenitors and cell line. *Biochem Biophys Res Commun*. 2011;405:128-133.
18. Lebbink RJ, de Ruiter T, Kaptijn GJ, Bihan DG, Jansen CA, Lenting PJ, Meyaard L. Mouse leukocyte-associated Ig-like receptor-1 (mLAIR-1) functions as an inhibitory collagen-binding receptor on immune cells. *Int Immunol*. 2007;19:1011-1019.
19. Kang X, Lu Z, Cui C, Deng M, Fan Y, Dong B, Han X, Xie F, Tyner JW, Coligan JE, Collins RH, Xiao X, You MJ, Zhang CC. The ITIM-containing receptor LAIR1 is essential for acute myeloid leukaemia development. *Nat Cell Biol*. 2015;17:665-677.

20. Chen Z, Shojaee S, Buchner M, et al. Signalling thresholds and negative B-cell selection in acute lymphoblastic leukaemia. *Nature*. 2015;521:357-361.
21. Mazharian A, Watson SP, Severin S. Critical role for ERK1/2 in bone marrow and fetal liver-derived primary megakaryocyte differentiation, motility, and proplatelet formation. *Exp Hematol*. 2009;37:1238-1249 e1235.
22. Shattil SJ, Newman PJ. Integrins: dynamic scaffolds for adhesion and signaling in platelets. *Blood*. 2004;104:1606-1615.
23. Dubois C, Panicot-Dubois L, Merrill-Skoloff G, Furie B, Furie BC. Glycoprotein VI-dependent and -independent pathways of thrombus formation in vivo. *Blood*. 2006;107:3902-3906.
24. Hoffmeister KM. The role of lectins and glycans in platelet clearance. *J Thromb Haemost*. 2011;9 Suppl 1:35-43.
25. Grozovsky R, Begonja AJ, Liu K, Visner G, Hartwig JH, Falet H, Hoffmeister KM. The Ashwell-Morell receptor regulates hepatic thrombopoietin production via JAK2-STAT3 signaling. *Nat Med*. 2015;21(1):47-54.
26. Josefsson EC, James C, Henley KJ, et al. Megakaryocytes possess a functional intrinsic apoptosis pathway that must be restrained to survive and produce platelets. *J Exp Med*. 2011;208:2017-2031.
27. Okada M. Regulation of the SRC family kinases by Csk. *Int J Biol Sci*. 2012;8:1385-1397.
28. Senis YA, Mazharian A, Mori J. Src family kinases: at the forefront of platelet activation. *Blood*. 2014;124:2013-2024.
29. Dhanjal TS, Pendaries C, Ross EA, Larson MK, Protty MB, Buckley CD, Watson SP. A novel role for PECAM-1 in megakaryocytokinesis and recovery of platelet counts in thrombocytopenic mice. *Blood*. 2007;109:4237-4244.

Highlights

- In this study, we show that deficiency of the ITIM-containing receptor LAIR-1 in megakaryocytes results in thrombocytosis and production of hyperactive platelets.

- We demonstrate that ablation of LAIR-1 in megakaryocytes leads to an increased Src family kinase activity and downstream signalling in response to collagen that is transmitted to platelets, rendering them hyper-reactive.

- As a consequence, we show that LAIR-1 KO mice exhibited increased thrombus formation following ferric chloride-induced carotid artery injury.

- Our findings reveal a novel function of the ITIM-containing receptor LAIR-1 in thrombopoiesis and provide further insight into the molecular mechanisms regulating megakaryocyte and platelet hyperactivity that could lead to a prothrombotic state.

Tables

Table 1: Megakaryocyte surface glycoprotein expression in LAIR-1 KO mice

Data represents mean values of the mean fluorescence intensity ± SEM, ***P < 0.001

Surface glycoproteins	WT (mean ± SEM; n = 6 - 10)	LAIR-1 KO (mean ± SEM; n = 6 - 10)	P value
GPVI	29 ± 2.7	27 ± 3.1	ns
Integrin α2	38 ± 1.7	40 ± 3.6	ns
GPIbα	34 ± 4.7	28 ± 5.6	ns
Integrin αIIbβ3	214 ± 10	215 ± 29	ns
CLEC-2	76 ± 5	68 ± 5.6	ns
G6b-B	25 ± 6	21 ± 5	ns
PECAM-1	330 ± 28	263 ± 14	ns
LAIR-1	6 ± 1.5	0.4 ± 1.1 ***	<0.001

Table 2: Platelet surface glycoprotein expression in LAIR-1 KO mice

Data represents mean values of the mean fluorescence intensity ± SEM

Surface glycoproteins	WT (mean ± SEM; n = 8 - 12)	LAIR-1 KO (mean ± SEM; n = 8 - 12)	P value
GPVI	1401 ± 118	1210 ± 82	ns
Integrin α2	821 ± 42	747 ± 52	ns
GPIbα	4305 ± 264	4260 ± 256	ns
Integrin αIIbβ3	3209 ± 111	3182 ± 167	ns
CLEC-2	6814 ± 205	6491 ± 466	ns
G6b-B	701 ± 77	902 ± 181	ns
PECAM-1	494 ± 35	535 ± 11	ns
LAIR-1	76 ± 10	72 ± 15	ns

Figure legends

Figure 1: LAIR-1 and GPVI are inversely expressed during megakaryopoiesis *in vitro*. (A) Expression of CD34, the collagen receptors LAIR-1, GPVI and $\alpha 2\beta 1$, and GPIbα and αIIbβ3 were measured at indicated days of *in vitro* murine megakaryopoiesis by flow cytometry. % of positive cells are represented, mean ± SEM n = 4-8. **(B)** Expressions of the collagen receptors LAIR-1, GPVI and $\alpha 2\beta 1$, and of the integrin αIIbβ3 were measured on day 0, 1, 5, 8 of *in vitro* murine megakaryopoiesis and in mouse platelets. Ploidy was evaluated in parallel. Representative histograms from three independent experiments are shown. Grey histograms represent isotype control staining and open histograms represent the different receptor staining. **(C) LAIR-1 is phosphorylated in primary mouse bone marrow-derived megakaryocytes.** Bone marrow-derived megakaryocytes were treated with 100 μM pervanadate (Perv), 30 μg/mL convulxin (Cvx) or with PBS alone for 15 minutes at 37°C and lysed with NP40 lysis buffer. Cell lysates were subjected to immunoprecipitation with anti-mouse LAIR-1 antibody coupled to protein G beads. Proteins were separated by SDS-PAGE and western blotted using anti-phosphotyrosine (upper panel) and anti-LAIR-1 (lower panel) antibodies. Representative blots from n = 3 independent experiments.

Figure 2: LAIR-1 KO mice exhibit a mild thrombocytosis. (Ai) Whole cell lysates of bone marrow-derived megakaryocytes and washed platelets from litter-matched wild-type (WT) and LAIR-1 knockout (KO) mice were western blotted with anti-mouse LAIR-1 antibody and tubulin as loading control. Representative western blots from n = 4 mice/genotype is represented. **(Aii)** Platelet counts and **(Aiii)** volumes from litter-matched WT (n = 38) and LAIR-1 KO mice *(*n = 36) were measured. Mean ± SEM; ***$P < 0.001$. **(B) Normal ultrastructure and organelle content of platelets from LAIR-1 KO mice.** Transmission electron micrographs of ultrathin sections platelets from litter-matched WT and LAIR-1 KO mice are shown. AG, α-granules; DG, dense granules; OCS, open canalicular system; M, mitochondria. **(C)** Platelet half-life was measured by flow cytometry after quantification of the number of biotin$^+\alpha$IIb$\beta 3^+$ platelets in the circulation of litter-matched WT and LAIR-1 KO mice daily pre-/post-injection of biotin-*N*-hydroxysuccinamide. Mean ± SEM n = 4-8 mice/genotype/time point; **$P < 0.01$; ***$P < 0.001$.

Figure 3: LAIR-KO mice exhibit normal megakaryocyte development but increased proplatelet formation. (A) Ploidy of bone marrow-derived megakaryocytes from litter-matched WT and LAIR-1 KO mice were quantified after propidium iodide staining by flow cytometry. **(Ai)** Representative profiles are shown; n = 4-6 mice/genotype. **(Aii)** The percentage of 2-128N ploidy cells was quantified. Mean ± SEM; n = 4-6 mice/genotype. **(B)** Bone marrow-derived megakaryocytes from litter-matched WT and LAIR-1 KO mice were plated on fibrinogen-coated surfaces for 3 hours. Images of spread megakaryocytes stained with Alexa-Fluor 568 phalloidin were taken. **(Bi)** Representative images (n = 4-6 mice/genotype) and **(Bii)** surface area mean ± SEM are shown. **(C)** Bone marrow-derived megakaryocytes from litter-matched WT and LAIR-1 KO mice were plated on fibrinogen-coated surfaces for 5 hours. **(Ci)** Representative images of proplatelet forming megakaryocytes stained with FITC-αIIbβ3 were taken. **(Cii)** Percent of

megakaryocytes forming proplatelets (n = 4-6 mice/genotype, mean ± SEM) and proplatelet mean areas are represented (**P < 0.01, scale bar: 20 μm).

Figure 4: Thrombopoietin and integrin, collagen signalling in LAIR-1-deficient megakaryocytes. (A) Bone marrow-derived megakaryocytes from litter-matched WT and LAIR-1 KO mice were stimulated with 50 ng/mL thrombopoietin (Tpo) for 10 minutes at 37°C. Whole cell lysates were western blotted with **(i)** anti-phospho-Erk1/2 (p-Erk1/2), anti-pan Erk1/2 (Erk1/2), and **(ii)** anti-Src p-Tyr418 and anti-pan Src antibodies. Representative blots and densitometry quantification from n = 3-5 independent experiments/genotype (mean ± SEM; *P < 0.05). **(B)** Bone marrow-derived megakaryocytes from litter-matched WT and LAIR-1 KO mice were plated on 100 μg/ml fibrinogen-coated surfaces for 3 hours at 37°C. Whole cell lysates were prepared of non-adherent (NA) and fibrinogen (fib) adherent megakaryocytes and were western blotted with **(Bi)** anti-phospho-Erk1/2 (p-Erk1/2), anti-pan Erk1/2 (Erk1/2), and **(Bii)** anti-Src p-Tyr418 and anti-pan Src antibodies. Representative blots and densitometry quantification from n = 3-5 independent experiments/genotype (mean ± SEM; *P < 0.05). **(C)** Bone marrow-derived megakaryocytes from litter-matched WT and LAIR-1 KO mice were stimulated with 30 μg/ml convulxin for 15 minutes at 37°C. Whole cell lysates were western blotted with anti-Src p-Tyr418, anti-Syk p-Tyr519/520 and anti-PLCγ2 p-Tyr1217 antibodies. Membranes were stripped and reblotted with anti-pan Src, anti-pan Syk and anti-pan PLCγ2 antibodies. **(Ci)** Representative blots and **(Cii)** densitometry quantification from n = 4 independent experiments/genotype (mean ± SEM; *P < 0.05, **P < 0.01).

Figure 5: Increased platelet reactivity in LAIR-1 KO mice. Platelet aggregation and ATP secretion of washed platelets were measured by lumi-aggregometery in response to **(Ai-iii)** 1, 3 and 10 μg/mL collagen, **(Bi-iii)** 1, 3 and 10 μg/mL collagen-related peptide (CRP)**, (Ci)** 0.06, 0.09 and 0.3 U/mL thrombin, **(Cii)** 0.25, 0.5 and 1 μM U46619 and **(Ciii)** 1, 3 and 10 μM ADP. Representative traces are shown, n = 4-8 mice/genotype/condition. Quantification of time to 25% platelet aggregation and ATP secretion in response to collagen **(Ai-iii)** and to CRP **(Bi-iii)** were measured. Mean ± SEM are represented (*P < 0.05, **P < 0.01). **(D)** P-selectin expression and fibrinogen binding of platelets from LAIR-1 KO mice in response to 1, 3 and 10 μg/mL CRP and 0.06 U/mL thrombin were measured. Geometric mean fluorescence intensity (MFI) ± SEM is represented; n = 3-5 mice/genotype; **P < 0.01.

Figure 6: Increased platelet spreading in LAIR-1 KO mice. (A) Basal and thrombin (0.1 U/mL)-activated platelets were plated on a fibrinogen-coated surface. **(Ai)** Representative differential interference contrast (DIC) and phalloidin-stained images of platelets. **(Aii)** Surface area of individual platelets in DIC images was measured; n = 3-5 mice/genotype, 250-500 platelets/condition; mean ± SEM; **P < 0.01; scale bar: 5 μm. **(B) Increased αIIbβ3 signalling in LAIR-1 KO mice.** Platelets from litter-matched WT and LAIR-1 KO mice were plated on 100 μg/mL fibrinogen-coated surfaces for 45 minutes at 37°C. Whole cell lysates were prepared of non-adherent (NA) and fibrinogen (fib) adherent platelets. **(Bi)** Equal amounts of total protein were resolved by SDS-PAGE and Western blotted with an anti-Src p-Tyr418, anti-Syk p-Tyr519/520 and anti-PLCγ2 p-Tyr1217. Membranes were subsequently stripped and reblotted with anti-Src, anti-Syk and anti-PLCγ2

antibodies. Blots are representative of 4 independent experiments. **(Bii)** Band intensities were quantified from 4 separate experiments (mean ± SEM; **P* < 0.05).

Figure 7: Increased GPVI-mediated signalling in platelets from LAIR-1 KO mice. (A) Whole cell lysates of resting and 1 μg/mL collagen-related peptide (CRP)-stimulated platelets from litter-matched WT and LAIR-1 KO mice were western blotted with anti-phosphotyrosine (p-Tyr) and anti-Src pTyr418 and membranes were stripped and reblotted with actin antibody. **(Ai)** Representative blots and **(Aii)** densitometry quantification from n = 3 independent experiments/genotype (mean ± SEM; **P* < 0.05, ***P* < 0.01). **(B)** Whole cell lysates of resting and 1 μg/mL CRP-stimulated platelets from litter-matched WT and LAIR-1 KO mice were western blotted with anti-Syk p-Tyr519/520, and anti-PLCγ2 p-Tyr1217 antibodies. Membranes were stripped and reblotted with anti-pan Syk and anti-pan PLCγ2 antibodies. **(Bi)** Representative blots and **(Bii)** densitometry quantification from n = 4 independent experiments/genotype (mean ± SEM; **P* < 0.05). **(C)** Anticoagulated blood was flowed through collagen-coated capillary tubes. DIC images of fixed platelets on collagen fibrils after being flowed through collagen-coated capillary tubes at 1,000 s^{-1} for 4 minutes. **(Ci)** Images are representative of 3 independent experiments. Scale bar: 10 μm. **(Cii)** Area covered by platelet thrombi was measured. Data presented are means (± SEM) of 3 independent experiments (***P* < 0.01). **(D) Laser injury-induced thrombus formation *in vivo*.** Mice were injected with Dylight488-conjugated anti-GPIbβ antibody (0.1 μg/g body weight, X488). Arterioles in cremaster muscles of recipients were subsequently injured by laser, and the accumulation of platelets (green) into the thrombi was assessed. **(Di)** Representative composite brightfield and fluorescence images from X488-labeled platelets after laser injury of arteriole are shown. Scale bar: 10 μm. **(Dii)** Each curve represents the median integrated thrombus fluorescence intensity in arbitrary units (a.u.) for 23-73 thrombi induced in 4-12 mice/genotype. See also supplementary videos SI and SII. **(E) Ferric chloride-induced thrombus formation *in vivo*.** Mice were injected with DyLight488-conjugated anti-GPIbβ antibody (0.1 μg/g body weight, X488). Exposed carotid arteries were injured with 10% ferric chloride for 3 minutes and the accumulation of platelets (green) into the thrombi was assessed. **(Ei)** Representative fluorescence images from X488-labeled platelets after ferric chloride injury of carotid are shown. Scale bar: 200 μm. **(Eii)** Each curve represents the median integrated fluorescence density in arbitrary units (a.u.) for 10 mice/genotype. **(Eiii)** Area under the curve of the integrated fluorescence density is represented (mean ± SEM; **P* < 0.05 using a Mann-Whitney test). See also supplementary videos SIII and SIV.

Materials and Methods

Mice

LAIR-1 knockout (KO) mice were generated by Taconic Artemis as shown in Supplemental Figure 1 and bred as heterozygotes. Wild-type (WT) littermates were used as controls. All procedures were undertaken with United Kingdom Home Office approval in accordance with the Animals (Scientific Procedures) Act of 1986.

Chemicals

Horm collagen was from Takeda (Munich, Germany). Convulxin was from Enzo Life Sciences (Exeter, UK). Human fibrinogen was from Enzyme Research Laboratories (Swansea, UK). FITC-conjugated rat-α-mouse GPVI, α2, αIIbβ3, GPIbα, P-selectin, phycoerythrin (PE)-conjugated JON/A, DyLight488-labeled anti-GPIbβ and rat IgG antibodies were from Emfret Analytics (Würzburg, Germany). Anti-mouse CD31-FITC was from BD Biosciences (San Jose, USA). Anti-mouse LAIR-1 purified and PE-conjugated antibodies and Armenian Hamster IgG Isotype controls were from eBioscience (Wembley, UK). FITC-conjugated anti-mouse CLEC2 and rat IgG antibodies were from Serotec (Kidlington, UK). The α-phospho-tyrosine (4G10) and PTP1B antibodies was from Millipore (Abingdon, UK). The α-Src-pY418, α-Src-pY529, pan Src were from Life Technologies (Paisley, UK). The α SykpY525/526, α-PLCγ2-pY1217, α-Lyn-pY507 antibodies were from Cell Signalling Technology (Hitchin, UK). The α Fyn-p-Y530 antibody was from Abcam (Cambridge, UK). The pan Lyn, pan Fyn, Csk, Shp1, Shp2 were from Santa Cruz Biotechnology (Heidelberg, UK). Horseradish peroxidase-conjugated secondary antibodies and ECL were purchased from Amersham Biosciences (GE Healthcare, Bucks, UK). All other reagents were purchased from Sigma-Aldrich (Poole, UK) or from sourced as previously described[1].

Platelet flow cytometry

Platelet surface glycoprotein expression was measured in whole blood using specific FITC-conjugated antibodies and analyzed with a FACSCalibur flow cytometer and CellQuest software (Becton Dickinson). Resting and activated platelets were fixed and stained with anti-P-selectin FITC-conjugated antibody or fibrinogen Alexa-Fluor 488 conjugated[2].

Platelet aggregation and secretion

Blood was collected from the inferior vena cava of CO_2-asphyxiated mice into 1/10 (v/v) acid-citrate-dextrose anticoagulant, and washed platelets (2×10^8/mL) were prepared[3]. Platelet aggregation and adenosine triphosphate (ATP) secretion were simultaneously measured using a lumi-aggregometer (Chrono-Log, Havertown, PA).

Platelet spreading

Washed platelets (2×10^7/mL) from LAIR-1 KO and litter-matched WT mice were either preincubated with or without 0.1 U/mL thrombin for 5 minutes and placed on 100 μg/mL fibrinogen-coated cover-slips, or placed on 100 μg/mL collagen-coated coverslips, for 45 minutes at 37°C[4]. Platelets were fixed with 4% formalin permeabilized with 0.1% Triton X-100 and stained with Alex Fluor 568-phalloidin. Images were captured by differential interference contrast (DIC) or confocal reflection microscopy and surface areas of platelets were measured using ImageJ software.

Platelet adhesion under flow

Blood was collected into 5 U/mL heparin and 40 μM PPACK (D-phenylalanyl-L-prolyl-L-arginine chloromethyl ketone), incubated for 10 minutes at 37°C with DiOC6 (3,3′-dihexyloxacarbocyanine iodide) and perfused through collagen-coated (100 μg/mL) glass microslide capillaries (1 × 0.1 mm) at 1,000 s^{-1} for 4 minutes at 37°C[3]. Capillaries were washed with modified Tyrode's for 5 min at 1000 s^{-1} and DIC images were captured.

Platelet biochemistry

Washed platelets (4 x 10^8/mL) were stimulated with 1 μg/ml collagen-related peptide (CRP) at 37°C with stirring at 1200 rpm in an aggregometer. Reactions were stopped with 2X SDS sample buffer to generate whole cell lysates (WCLs). For integrin signaling, coverslips were coated with fibrinogen (100 μg/mL) overnight at 4°C, blocked with denatured BSA (5 mg/mL) for 1 hour at room temperature, and washed with PBS before use. Platelets were plated on fibrinogen for 45 minutes at 37°C. Non-adherent platelets were removed and lysed by addition of 2X lysis buffer (basal). Adherent platelets were washed twice with Tyrode's buffer then lysed with 1X lysis buffer, incubated on ice for 10 minutes before scraping. Equal amount of proteins were resolved on 4-12% NuPAGE Bis-Tris gradient gels and immunoblotted with primary antibodies and horseradish peroxidase-conjugated secondary antibody. Proteins were detected by enhanced chemiluminescence and autoradiography[2].

Preparation and culture of mouse megakaryocytes

Bone marrow-derived megakaryocytes from LAIR-1 KO and litter-matched WT mice were cultured as previously described[1,5,6]. Different stages of megakaryocyte maturation were identified by their ploidy profile and expression level of glycoproteins. Throughout the study, we have used the subset of megakaryocytes which expresses both GPVI and LAIR-1.

Megakaryocyte ploidy and surface receptor expression

Surface receptor expression of αIIbβ3, GPIbα, GPVI and integrin α2β1, CLEC-2, G6b-B, PECAM-1 and LAIR-1 were measured on cultured bone marrow-derived megakaryocytes by flow cytometry with FITC-conjugated primary antibodies during megakaryocyte differentiation. The DNA ploidy of megakaryocytes isolated by BSA gradient was analysed after anti-αIIbβ3 staining and DNA staining with propidium iodide (10 μg/mL). Cells positive for αIIbβ3 were gated to analyse DNA content as described[5].

Megakaryocyte spreading and proplatelet formation *in vitro*

Coverslips were coated with fibrinogen (100 μg/mL) or collagen (100 μg/mL) overnight at 4°C, blocked with denatured BSA (5 mg/mL) for 1 hour at room temperature, and washed with PBS before use. Megakaryocytes were plated on a fibrinogen or collagen-coated surface for 3 (spreading) or 5 (proplatelet formation) hours at 37°C. Adherent megakaryocytes were fixed with 4% formalin and permeabilized with 0.1% Triton X-100. Actin fibres were stained with Alex Fluor 568-phalloidin and megakaryocytes forming proplatelets with anti–mouse αIIbβ3-FITC antibody as described[5].

Megakaryocyte biochemistry
Megakaryocytes were starved for 4 hours at 37°C in serum-free media following *ex vivo* differentiation and BSA gradient. Whole-cell lysates were prepared from megakaryocytes stimulated for 10 minutes with 50 ng/mL thrombopoietin (Tpo) or from non-adherent and fibrinogen adherent megakaryocytes for 3 hours. Equal amount of proteins were resolved on 4-12% NuPAGE Bis-Tris gradient gels and immunoblotted with primary antibodies and horseradish peroxidase-conjugated secondary antibody. Proteins were detected by enhanced chemiluminescence and autoradiography[2].

Immunohistochemistry
Femora and spleens from LAIR-1 KO and litter-matched WT mice were fixed in buffered formalin and embedded in paraffin. Sections (5 μm) were stained with haematoxylin and eosin (H&E) and reticulin and examined with a Zeiss Axiovert 200 inverted microscope using a 40X objective.

Tail bleeding assay
Blood loss was measured in anaesthetized 8-10 week old LAIR-1 KO mice and litter-matched WT following excision of a 3 mm portion of the tail tip, as previously described[2]. Mice were allowed to bleed until they lost either 15% blood volume (assuming a blood volume of 70 mL/kg) or for 30 minutes. Normalized blood loss was determined by lost blood/body weight.

Platelet half-life
Whole blood was collected at various times post-intravenous injection of 150 μL of 4 mg/mL N-hydroxysuccinimide ester (NHS)-biotin and percentage of biotin-labeled platelets was determined by flow cytometry, as described[7].

Clot retraction
For clot retraction studies, 400 μL PRP, adjusted to a concentration of 3×10^8 platelets/μL, were supplemented with 2 mM $CaCl_2$ and fibrinogen 2 mg/mL. Clotting was induced by addition of high thrombin concentrations (10 U/mL)[8]. Subsequent clot retraction was monitored at 37°C under non-stirring conditions and percentage of extruded serum was monitored at different time points.

Laser-induced thrombus formation model
Experiments were conducted on 20- to 25g LAIR-1 KO and litter-matched WT mice, as previously described[9]. Mice were anesthetized intraperitoneally with Avertin (240 μg/g body weight, 2,2,2-Tribromoethanol, Sigma-Aldrich). The cremaster muscle surrounding the testicle was exteriorized and spread flat over an optically clear coverslip on a pedestal and continuously superfused with a bicarbonate-buffered saline (pH 7.4; 37°C) gassed with 5% CO_2/95% N_2. Mice were injected with DyLight488-conjugated anti-GPIbβ antibody (0.1 μg/g body weight, X488) via the carotid artery. Laser-induced thrombi were generated at the luminal surface of selected arterioles, as previously described[10]. Real-time intravital brightfield and fluorescent images of the developing thrombus were captured simultaneously by confocal microscopy and analysed using Slidebook6 software (Intelligent Imaging Innovations).

Ferric chloride-induced thrombus formation model

Experiments were conducted on 20- to 30g LAIR-1 KO and litter-matched WT mice, as previously described[10]. Mice were anesthetized intraperitoneally with Avertin (240 μg/g body weight, 2,2,2-Tribromoethanol, Sigma-Aldrich). Platelets were labelled by intravenous administration of DyLight488-conjugated anti-GPIbβ antibody (0.1 μg/g body weight, X488). Right carotid arteries were exposed and filter paper (2 x 1 mm) soaked with 10% ferric chloride in PBS was applied for 3 minutes on the arterial adventitia. Injury sites were imaged by time-lapse microscopy for 15 minutes, and images were analysed using Slidebook6 software (Intelligent Imaging Innovations). Background fluorescence values measured upstream of the injury site were subtracted from the thrombus-specific fluorescence. Data are expressed as integrated fluorescence density.

Statistical analysis

Statistical significance was analysed using the unpaired Student's t-test . $P < 0.05$ was considered statistically significant.

References

1. Mazharian A, Ghevaert C, Zhang L, Massberg S, Watson SP. Dasatinib enhances megakaryocyte differentiation but inhibits platelet formation. *Blood*. 2011;117:5198-5206.
2. Senis YA, Tomlinson MG, Ellison S, et al. The tyrosine phosphatase CD148 is an essential positive regulator of platelet activation and thrombosis. *Blood*. 2009;113:4942-4954.
3. Senis YA, Atkinson BT, Pearce AC, et al. Role of the p110delta PI 3-kinase in integrin and ITAM receptor signalling in platelets. *Platelets*. 2005;16:191-202.
4. McCarty OJ, Larson MK, Auger JM, et al. Rac1 is essential for platelet lamellipodia formation and aggregate stability under flow. *J. Biol. Chem*. 2005;280:39474-39484.
5. Mazharian A, Watson SP, Severin S. Critical role for ERK1/2 in bone marrow and fetal liver-derived primary megakaryocyte differentiation, motility, and proplatelet formation. *Exp. Hematol*. 2009;37:1238-1249 e1235.
6. Dumon S, Heath VL, Tomlinson MG, Gottgens B, Frampton J. Differentiation of murine committed megakaryocytic progenitors isolated by a novel strategy reveals the complexity of GATA and Ets factor involvement in megakaryocytopoiesis and an unexpected potential role for GATA-6. *Exp. Hematol*. 2006;34:654-663.
7. Ault KA, Knowles C. In vivo biotinylation demonstrates that reticulated platelets are the youngest platelets in circulation. *Exp. Hematol*. 1995;23:996-1001.
8. Dhanjal T, Ross EA, Auger JM, McCarty OJ, Hughes CE, Senis YA, Buckley CD, Watson SP. Minimal regulation of platelet activity by PECAM-1. Platelets. 2007; 18:56-57.
9. Kalia N, Auger JM, Atkinson B, Watson SP. Critical role of FcR γ-chain, LAT, PLCγ2 and thrombin in arteriolar thrombus formation upon mild, laser induced endothelial injury in vivo. *Microcirculation*. 2008; 15:325-335.
10. Williams CM, Harper MT, Goggs R, Walsh TG, Offermanns S, Poole AW. Leukemia-associated Rho guanine-nucleotide exchange factor is not critical

for RhoA regulation, yet is important for platelet activation and thrombosis in mice. *J. Thromb. Haemost.* 2015; 13:2102-2107.

Figure 1

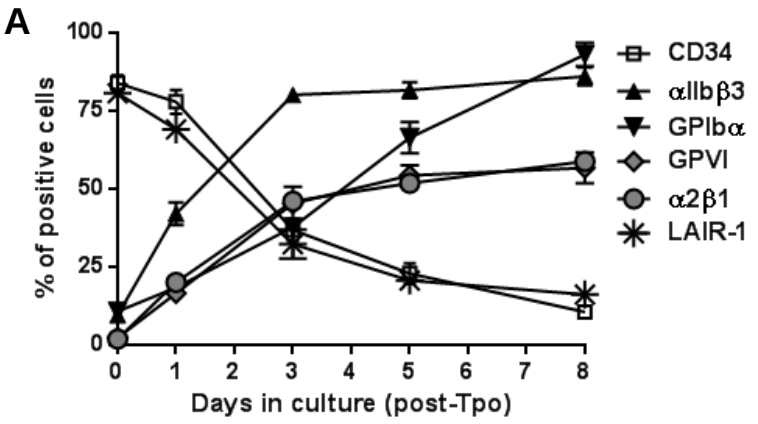
A
100
75
50
25
0
% of positive cells
0 1 2 3 4 5 6 7 8
Days in culture (post-Tpo)
CD34
αIIbβ3
GPIbα
GPVI
α2β1
LAIR-1

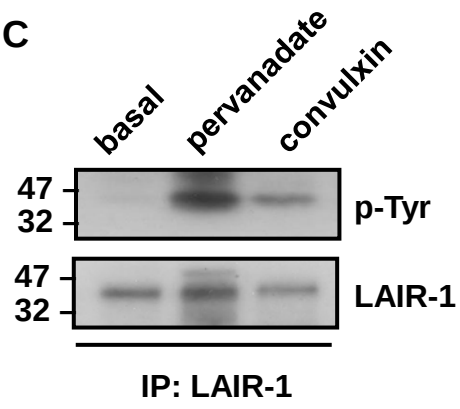
C
basal
pervanadate
convulxin
47
32
p-Tyr
47
32
LAIR-1
IP: LAIR-1

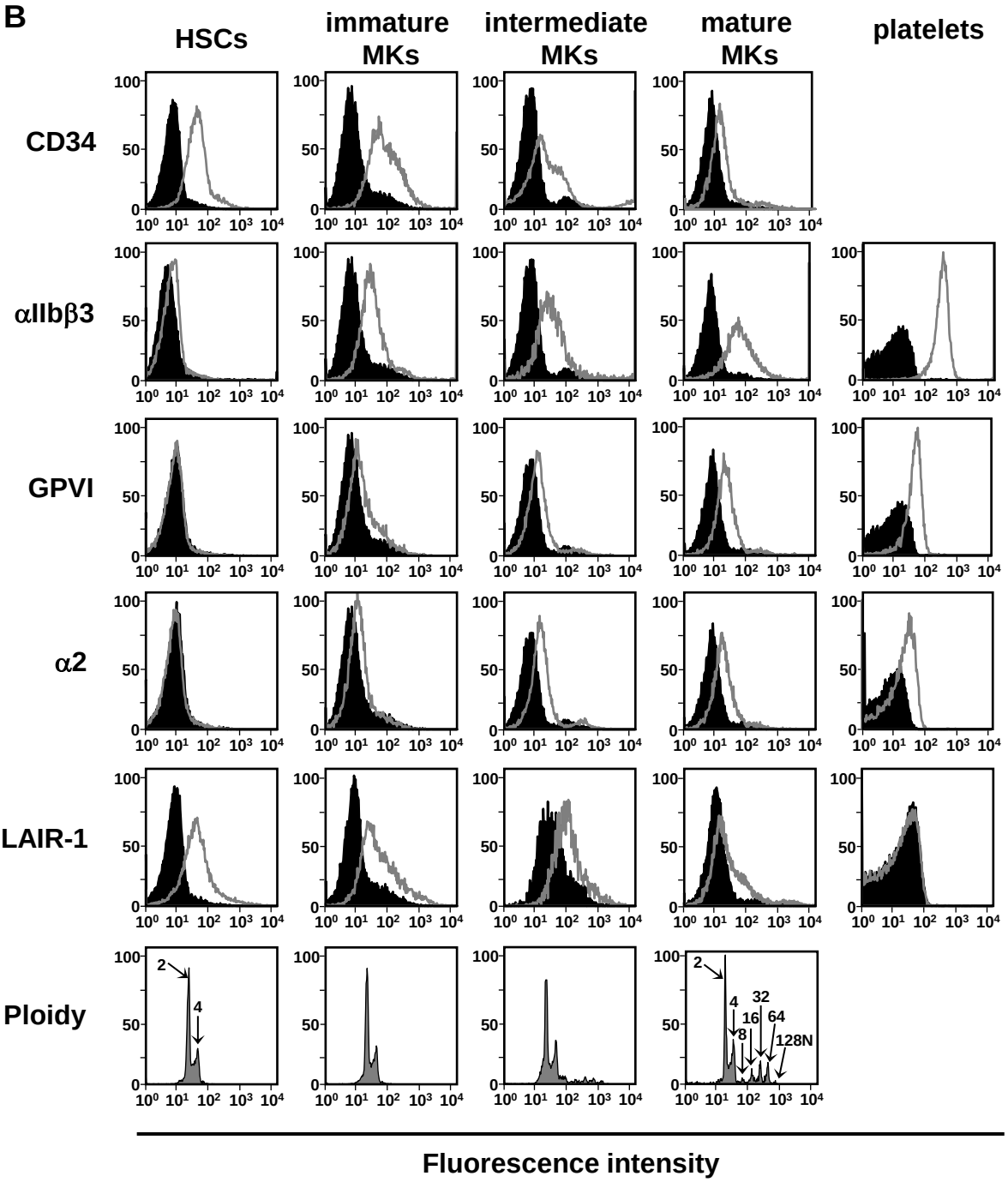
B
HSCs
immature MKs
intermediate MKs
mature MKs
platelets
CD34
αIIbβ3
GPVI
α2
LAIR-1
Ploidy
2
4
2
4
8
16
32
64
128N
Fluorescence intensity

Figure 2

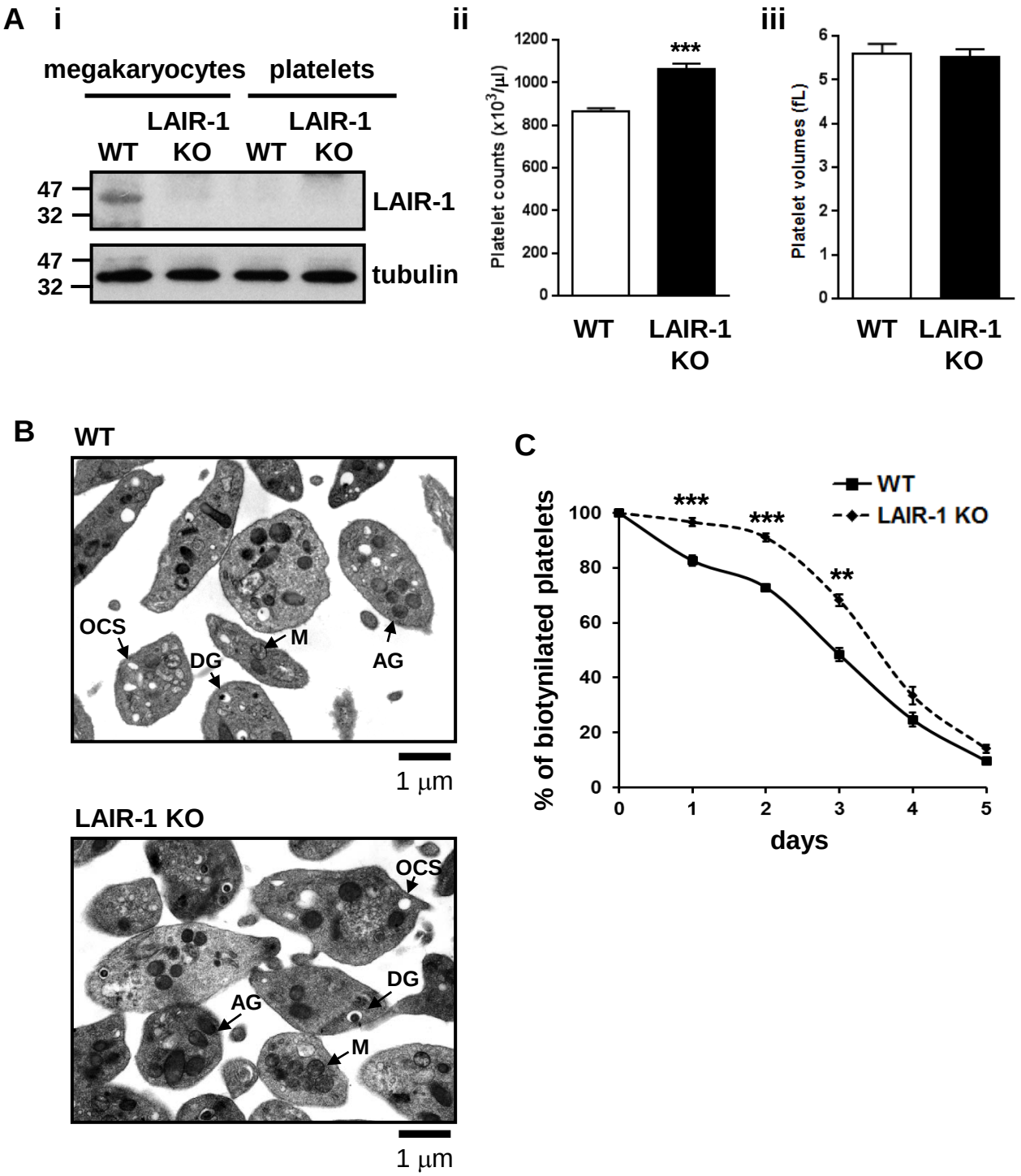
A i
megakaryocytes
platelets
LAIR-1
LAIR-1
WT
KO
WT
KO
47
32
LAIR-1
47
32
tubulin
ii
Platelet counts (x10³/μl)
1200
1000
800
600
400
200
0
***
WT
LAIR-1 KO
iii
Platelet volumes (fL)
6
5
4
3
2
1
0
WT
LAIR-1 KO
B
WT
OCS
M
DG
AG
1 μm
LAIR-1 KO
OCS
DG
AG
M
1 μm
C
% of biotynilated platelets
100
80
60
40
20
0
***
***
**
WT
LAIR-1 KO
0
1
2
3
4
5
days

Figure 3

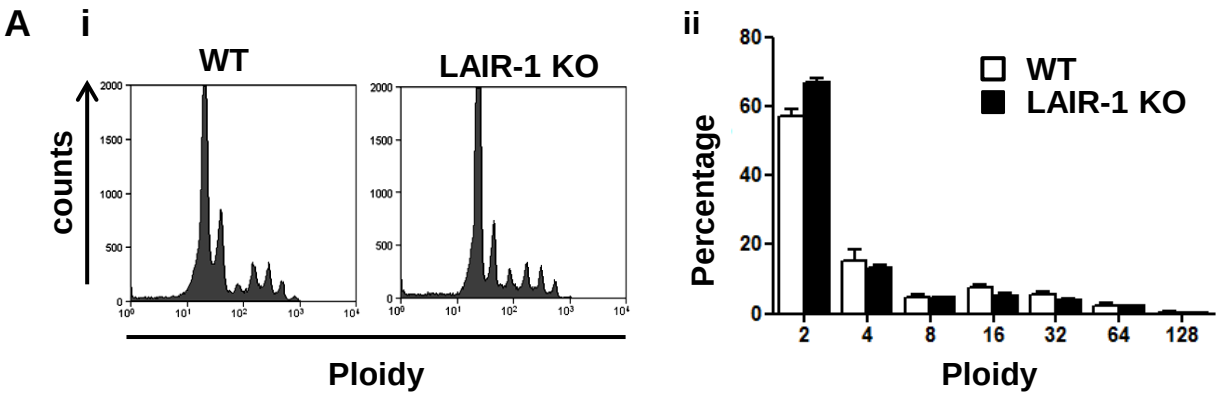
A
i
WT
LAIR-1 KO
counts
Ploidy
ii
WT
LAIR-1 KO
Percentage
Ploidy
2
4
8
16
32
64
128

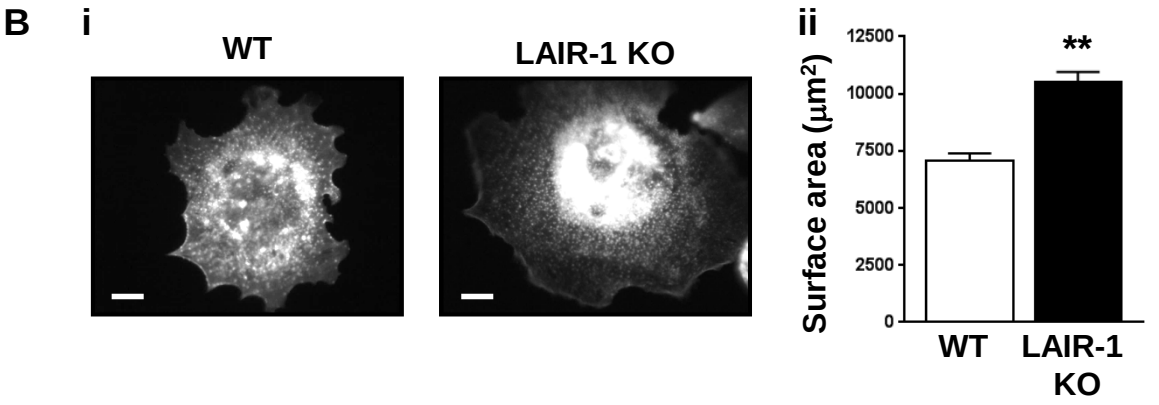
B
i
WT
LAIR-1 KO
ii
Surface area (μm²)
**
WT
LAIR-1 KO

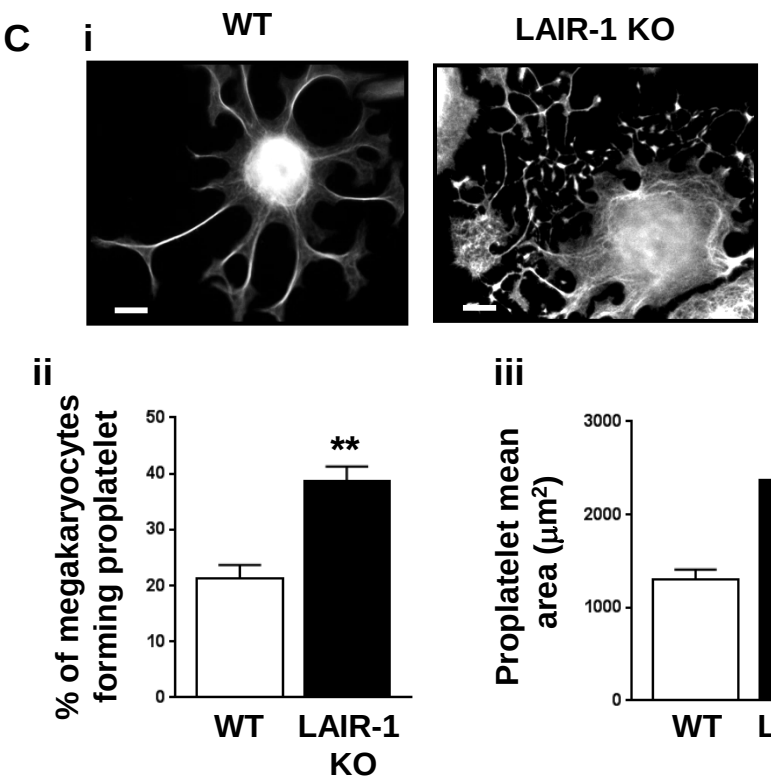
C
i
WT
LAIR-1 KO
ii
% of megakaryocytes forming proplatelet
**
WT
LAIR-1 KO
iii
Proplatelet mean area (μm²)
**
WT
LAIR-1 KO

Figure 4

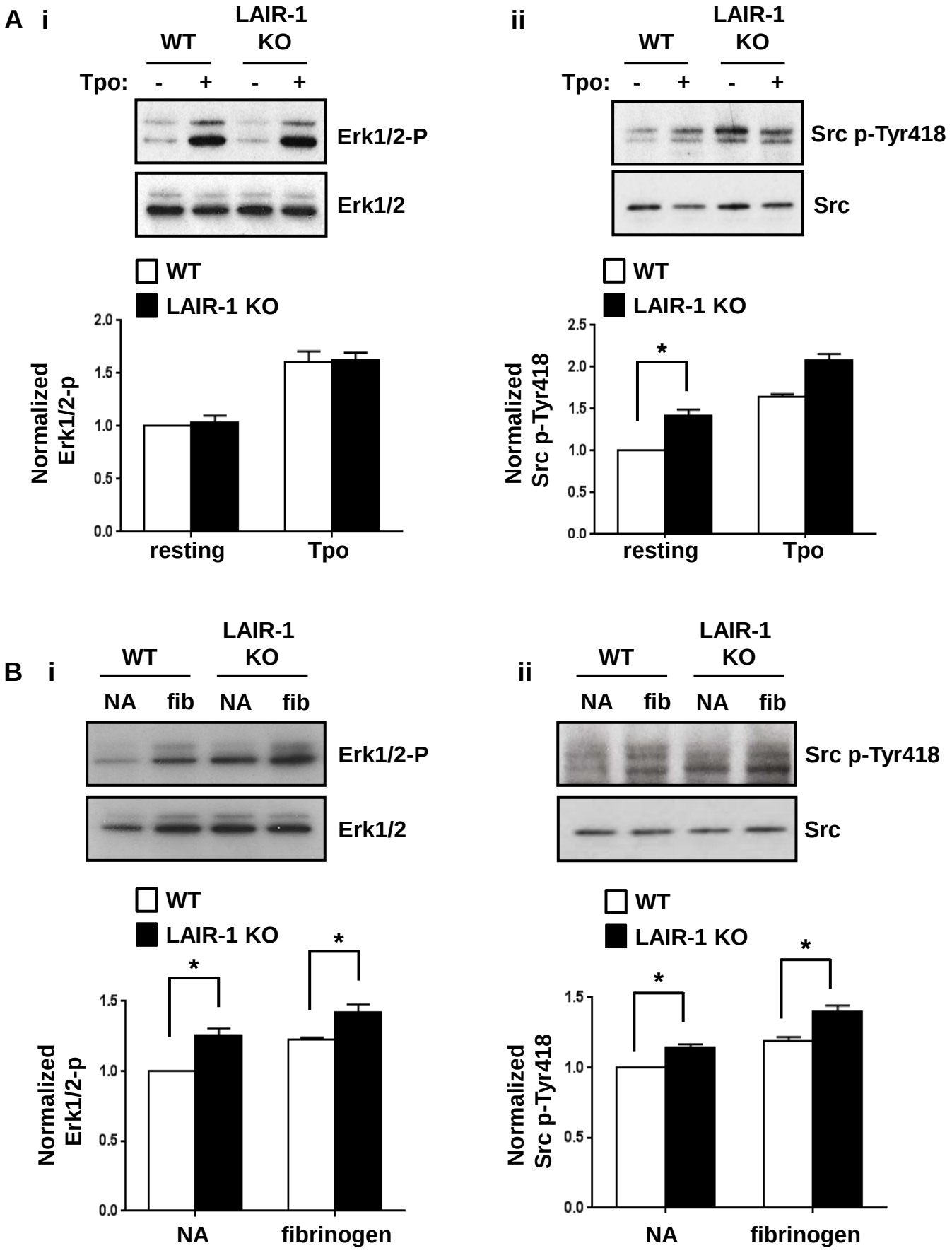
A i
LAIR-1
WT
KO
Tpo: - + - +
Erk1/2-P
Erk1/2
WT
LAIR-1 KO
Normalized Erk1/2-p
2.0
1.5
1.0
0.5
0.0
resting
Tpo
ii
LAIR-1
WT
KO
Tpo: - + - +
Src p-Tyr418
Src
WT
LAIR-1 KO
Normalized Src p-Tyr418
2.5
2.0
1.5
1.0
0.5
0.0
*
resting
Tpo
B i
LAIR-1
WT
KO
NA fib NA fib
Erk1/2-P
Erk1/2
WT
LAIR-1 KO
*
Normalized Erk1/2-p
1.5
1.0
0.5
0.0
*
NA
fibrinogen
ii
LAIR-1
WT
KO
NA fib NA fib
Src p-Tyr418
Src
WT
LAIR-1 KO
*
Normalized Src p-Tyr418
1.5
1.0
0.5
0.0
*
NA
fibrinogen

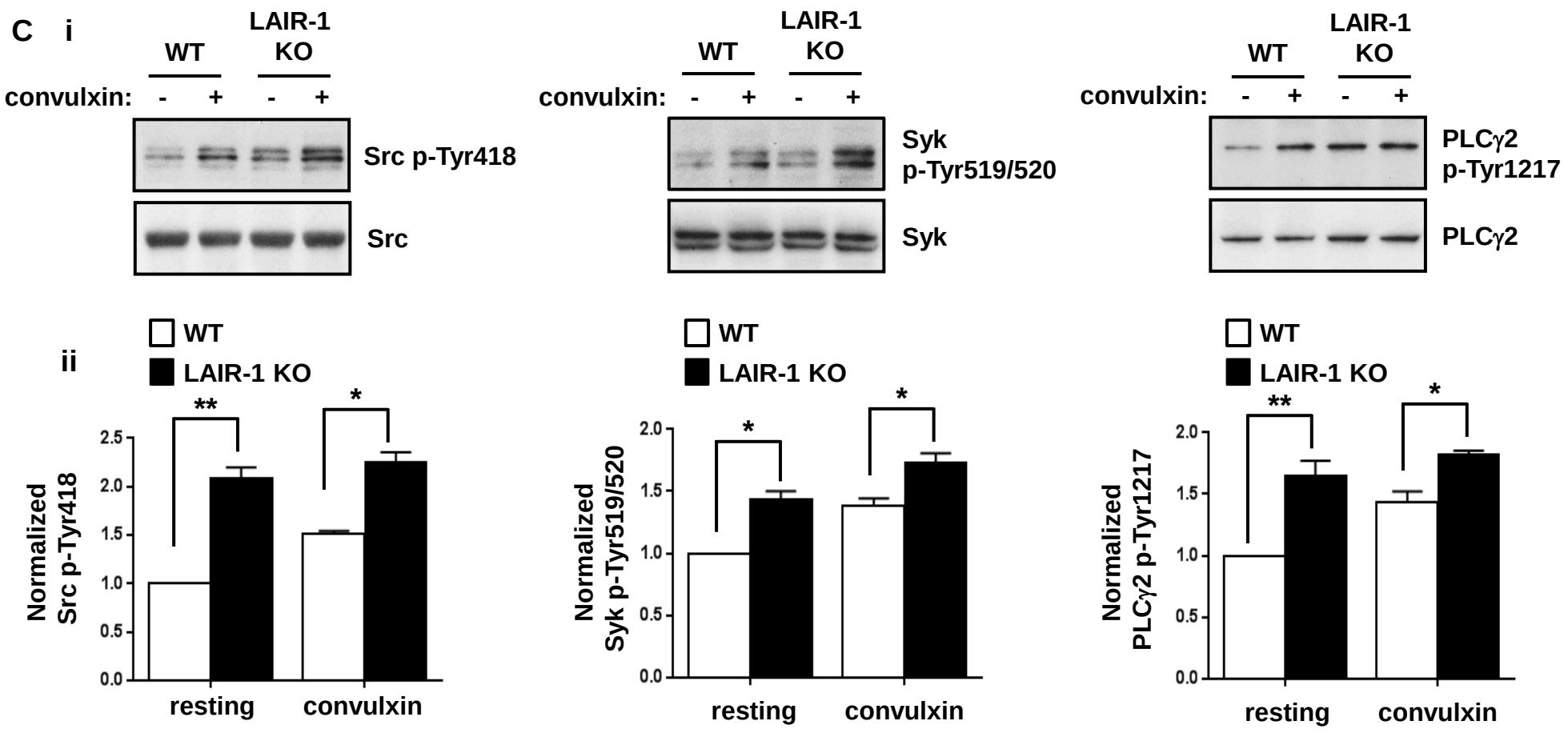
C i
LAIR-1
WT
KO
convulxin: - + - +
Src p-Tyr418
Src
Syk p-Tyr519/520
Syk
PLCγ2 p-Tyr1217
PLCγ2
ii
WT
LAIR-1 KO
**
*
Normalized Src p-Tyr418
2.5
2.0
1.5
1.0
0.5
0.0
resting
convulxin
Normalized Syk p-Tyr519/520
Normalized PLCγ2 p-Tyr1217

Figure 5

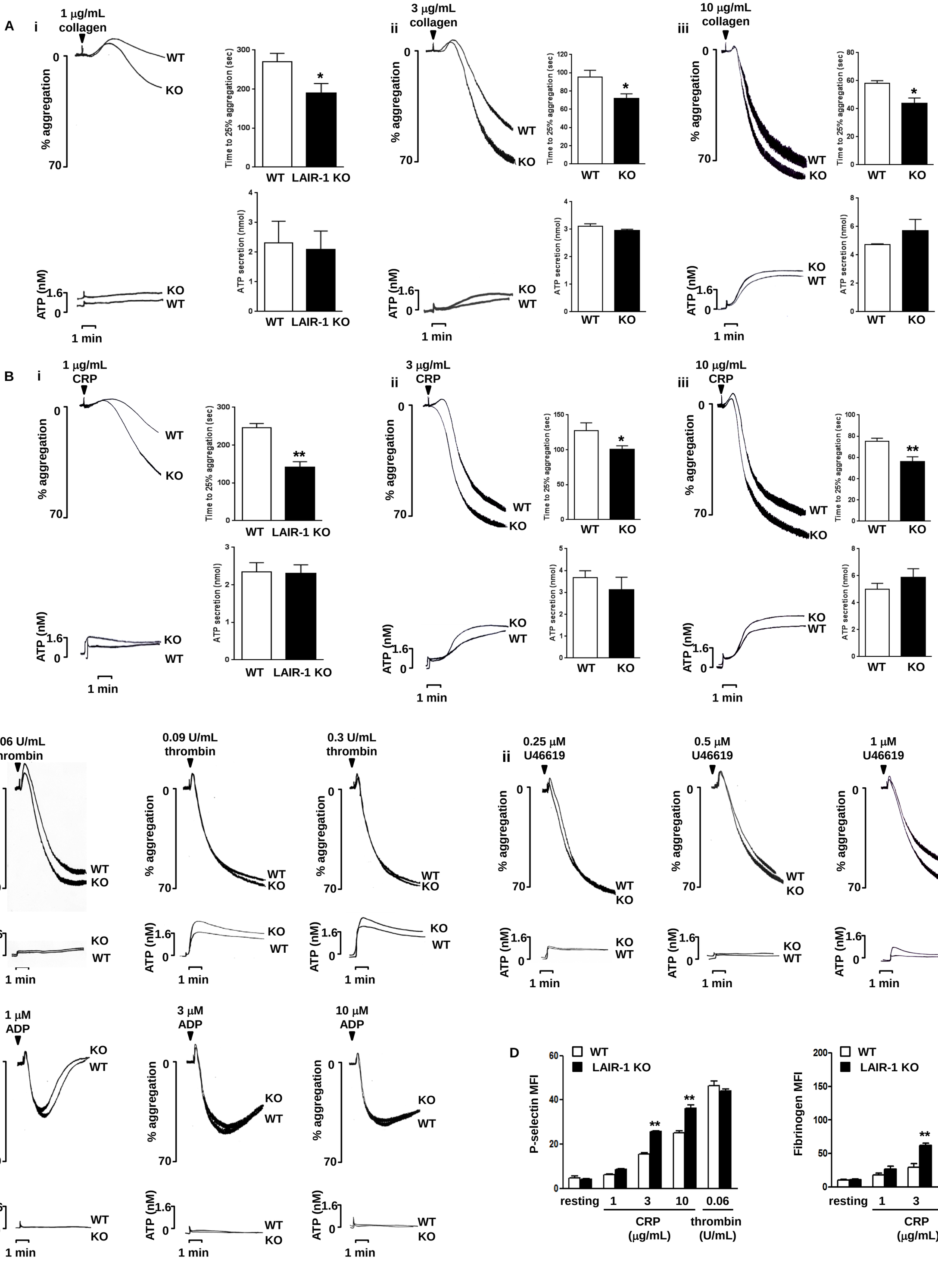
A
i
1 μg/mL collagen
% aggregation
0
70
WT
KO
Time to 25% aggregation (sec)
300
200
100
0
*
WT LAIR-1 KO
ATP (nM)
1.6
0
KO
WT
1 min
ATP secretion (nmol)
4
3
2
1
0
WT LAIR-1 KO
ii
3 μg/mL collagen
% aggregation
0
70
WT
KO
Time to 25% aggregation (sec)
120
100
80
60
40
20
0
*
WT KO
ATP (nM)
1.6
0
KO
WT
1 min
ATP secretion (nmol)
4
3
2
1
0
WT KO
iii
10 μg/mL collagen
% aggregation
0
70
WT
KO
Time to 25% aggregation (sec)
80
60
40
20
0
*
WT KO
ATP (nM)
1.6
0
KO
WT
1 min
ATP secretion (nmol)
8
6
4
2
0
WT KO
B
i
1 μg/mL CRP
% aggregation
0
70
WT
KO
Time to 25% aggregation (sec)
300
200
100
0
**
WT LAIR-1 KO
ATP (nM)
1.6
0
KO
WT
1 min
ATP secretion (nmol)
3
2
1
0
WT LAIR-1 KO
ii
3 μg/mL CRP
% aggregation
0
70
WT
KO
Time to 25% aggregation (sec)
150
100
50
0
*
WT KO
ATP (nM)
1.6
0
KO
WT
1 min
ATP secretion (nmol)
5
4
3
2
1
0
WT KO
iii
10 μg/mL CRP
% aggregation
0
70
WT
KO
Time to 25% aggregation (sec)
100
80
60
40
20
0
**
WT KO
ATP (nM)
1.6
0
KO
WT
1 min
ATP secretion (nmol)
8
6
4
2
0
WT KO
C
i
0.06 U/mL thrombin
0.09 U/mL thrombin
0.3 U/mL thrombin
ii
0.25 μM U46619
0.5 μM U46619
1 μM U46619
% aggregation
0
70
WT
KO
ATP (nM)
1.6
0
KO
WT
1 min
iii
1 μM ADP
3 μM ADP
10 μM ADP
% aggregation
0
70
KO
WT
ATP (nM)
1.6
0
WT
KO
1 min
D
P-selectin MFI
60
40
20
0
WT
LAIR-1 KO
**
resting 1 3 10 0.06
CRP (μg/mL)
thrombin (U/mL)
Fibrinogen MFI
200
150
100
50
0
WT
LAIR-1 KO
**
resting 1 3 10 0.06
CRP (μg/mL)
thrombin (U/mL)

Figure 6

A i

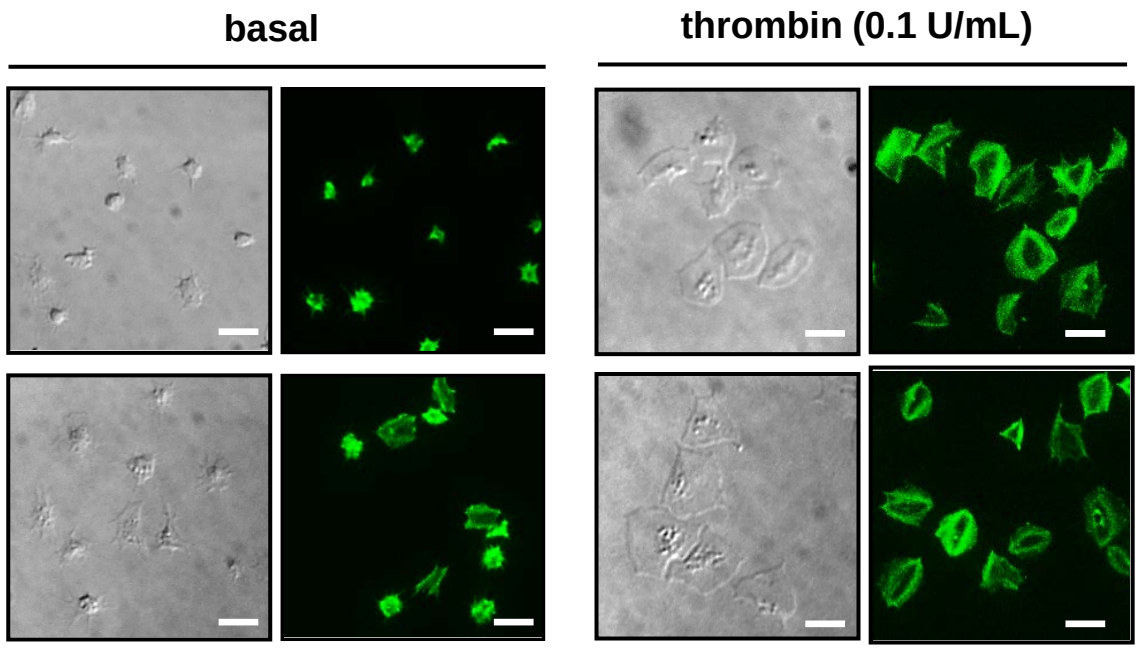

ii

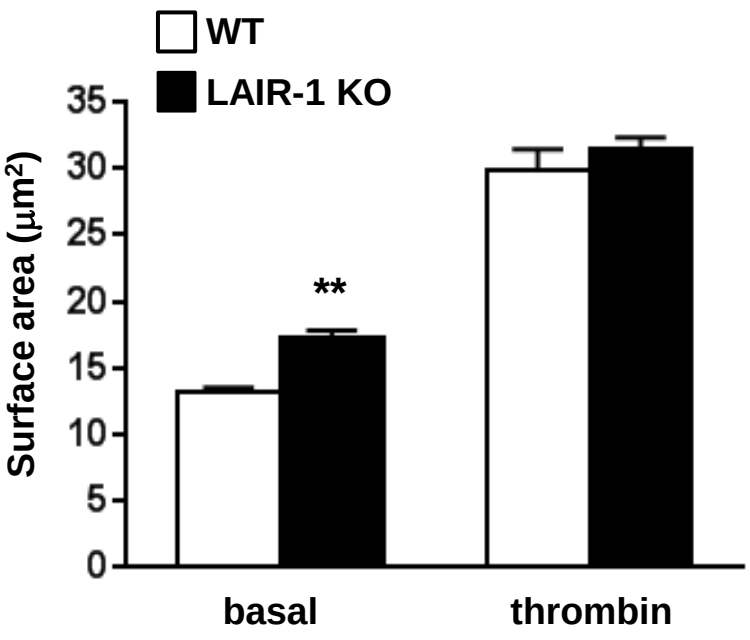

B i

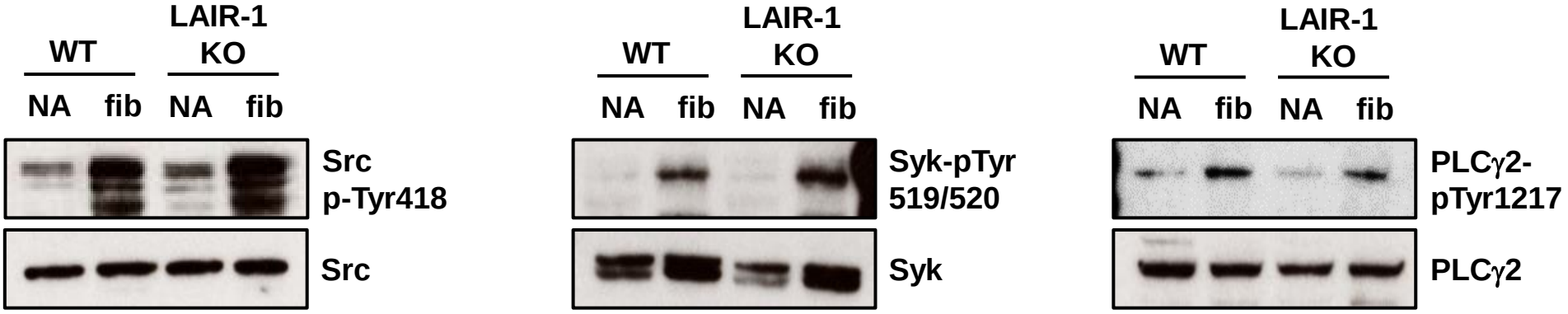

ii

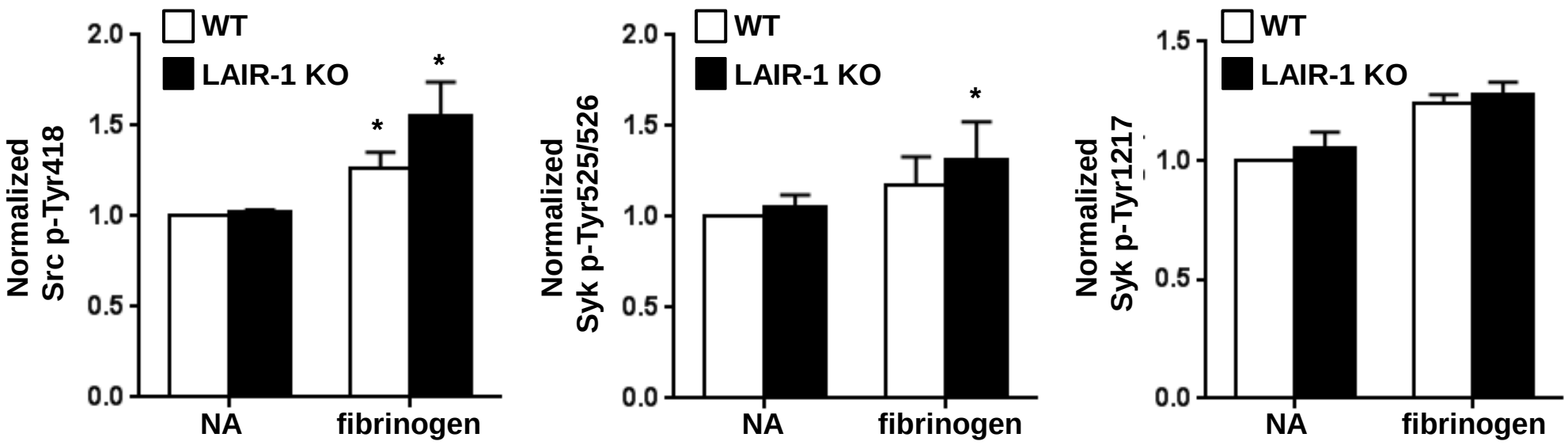

Figure 7

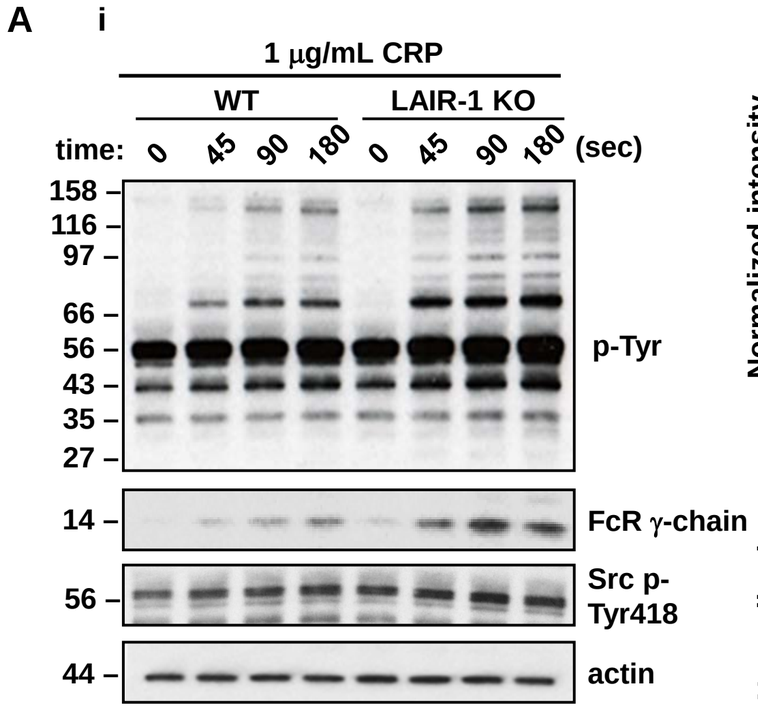
A
i
1 μg/mL CRP
WT
LAIR-1 KO
time: 0 45 90 180 0 45 90 180 (sec)
158
116
97
66
56
43
35
27
p-Tyr
14
FcR γ-chain
56
Src p-Tyr418
44
actin

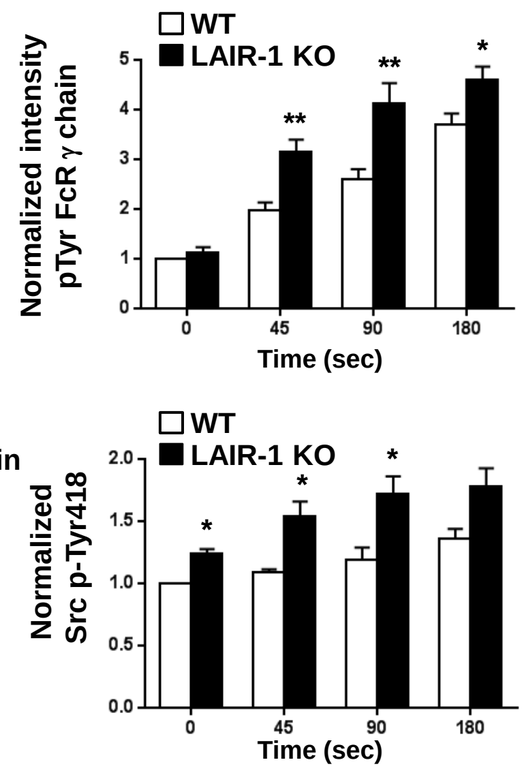
ii
WT
LAIR-1 KO
Normalized intensity pTyr FcR γ chain
Time (sec)
Normalized Src p-Tyr418
Time (sec)

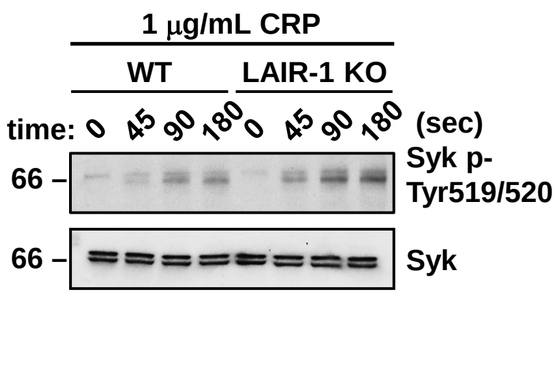
B
i
1 μg/mL CRP
WT
LAIR-1 KO
time: 0 45 90 180 0 45 90 180 (sec)
66
Syk p-Tyr519/520
66
Syk
1 μg/mL CRP
WT
LAIR-1 KO
time: 0 45 90 180 0 45 90 180 (sec)
158
PLCγ2 p-Tyr1217
158
PLCγ2

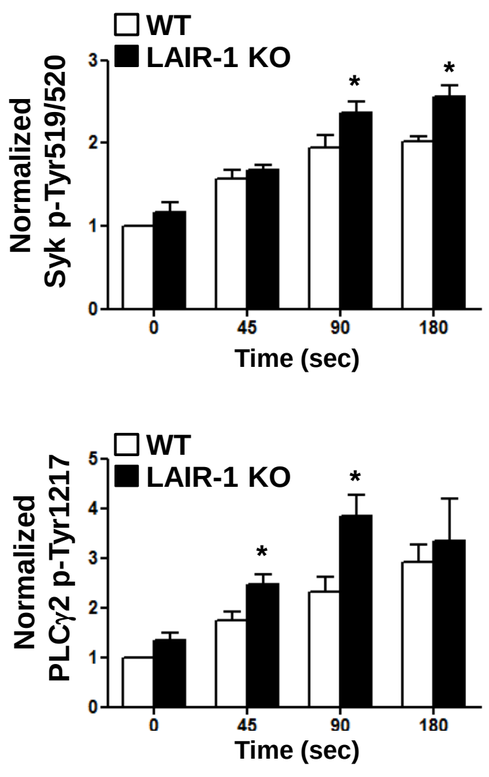
ii
WT
LAIR-1 KO
Normalized Syk p-Tyr519/520
Time (sec)
Normalized PLCγ2 p-Tyr1217
Time (sec)

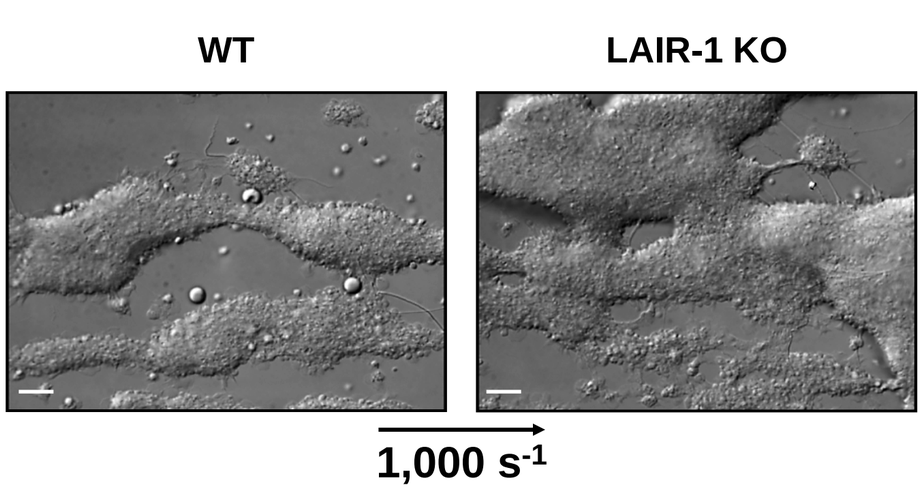
C
i
WT
LAIR-1 KO
1,000 s-1

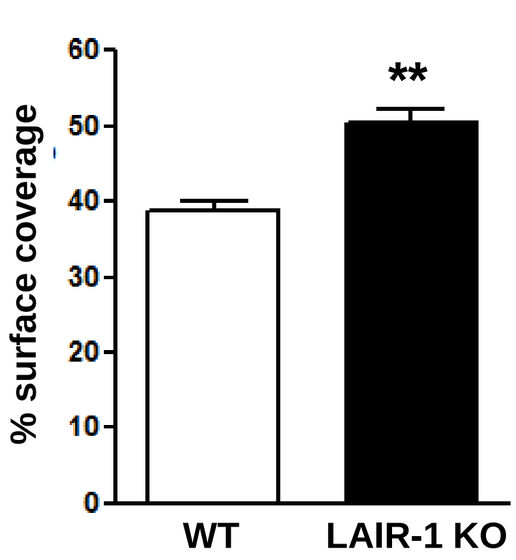
ii
% surface coverage
WT
LAIR-1 KO

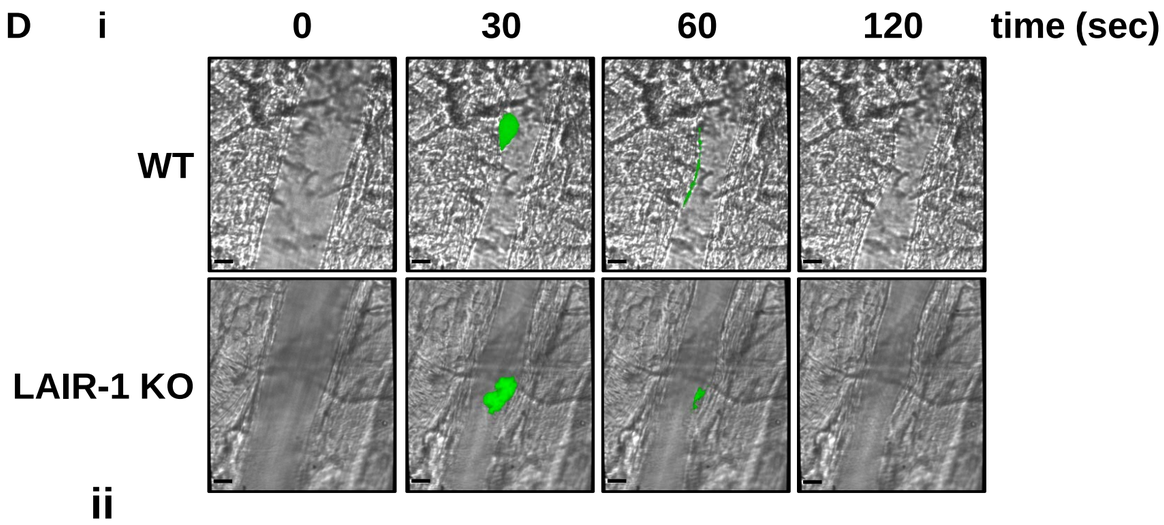
D
i
0
30
60
120
time (sec)
WT
LAIR-1 KO
ii
Thrombus fluorescence intensity (a.u.)
WT
LAIR-1 KO
Time (seconds)

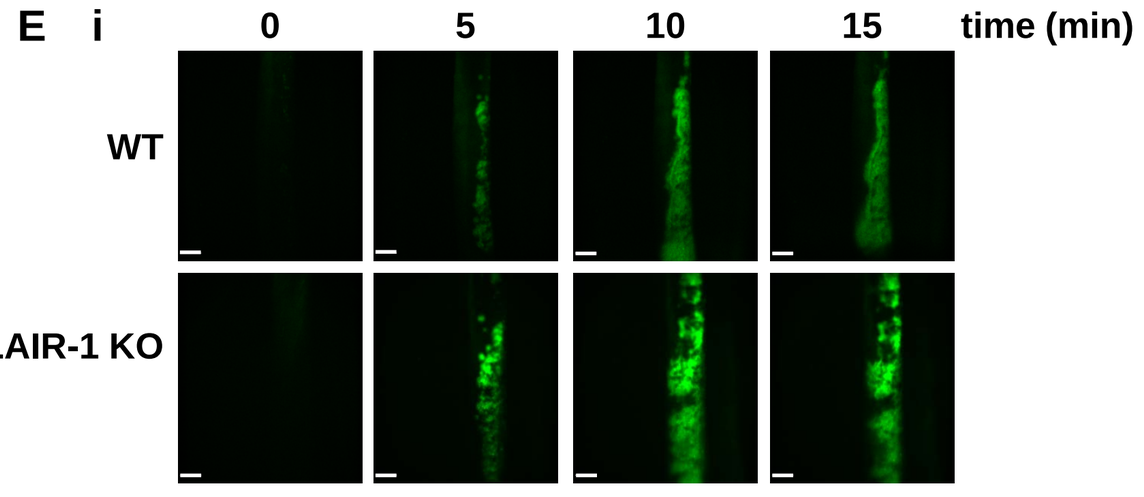
E
i
0
5
10
15
time (min)
WT
LAIR-1 KO

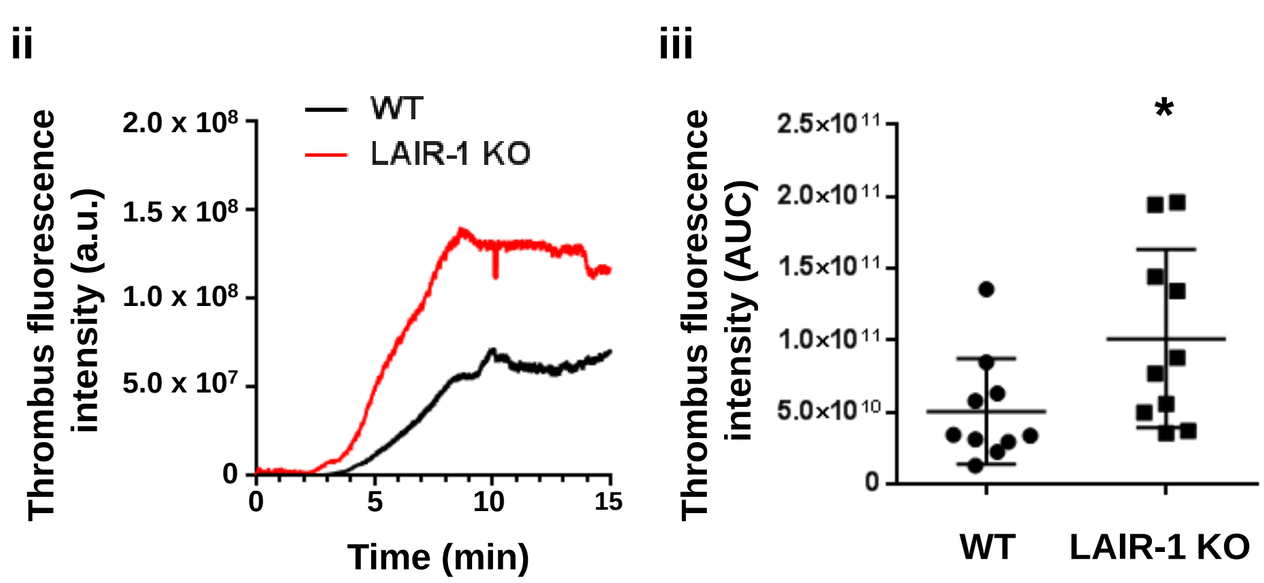
ii
Thrombus fluorescence intensity (a.u.)
WT
LAIR-1 KO
Time (min)
iii
Thrombus fluorescence intensity (AUC)
WT
LAIR-1 KO

Supplemental Material

Mice lacking the inhibitory collagen receptor leukocyte-associated immunoglobulin-like receptor-1 exhibit a mild thrombocytosis and hyperactive platelets

Christopher Smith[1], Steven G. Thomas[1], Zaher Raslan[1], Pushpa Patel[1], Maxwell Byrne[1], Marie Lordkipanidzé[1], Danai Bem[2], Linde Meyaard[3], Yotis A. Senis[1] and Steve P. Watson[1] and Alexandra Mazharian[1]

[1]Institute of Cardiovascular Sciences, College of Medical and Dental Sciences, University of Birmingham, Birmingham, B15 2TT, United Kingdom. [2]Institute of Applied Health Research, College of Medical and Dental Sciences, University of Birmingham, Birmingham, B15 2TT, United Kingdom. [3]Laboratory of Translational Immunology, Department of Immunology, University Medical Center Utrecht, Utrecht, The Netherlands.

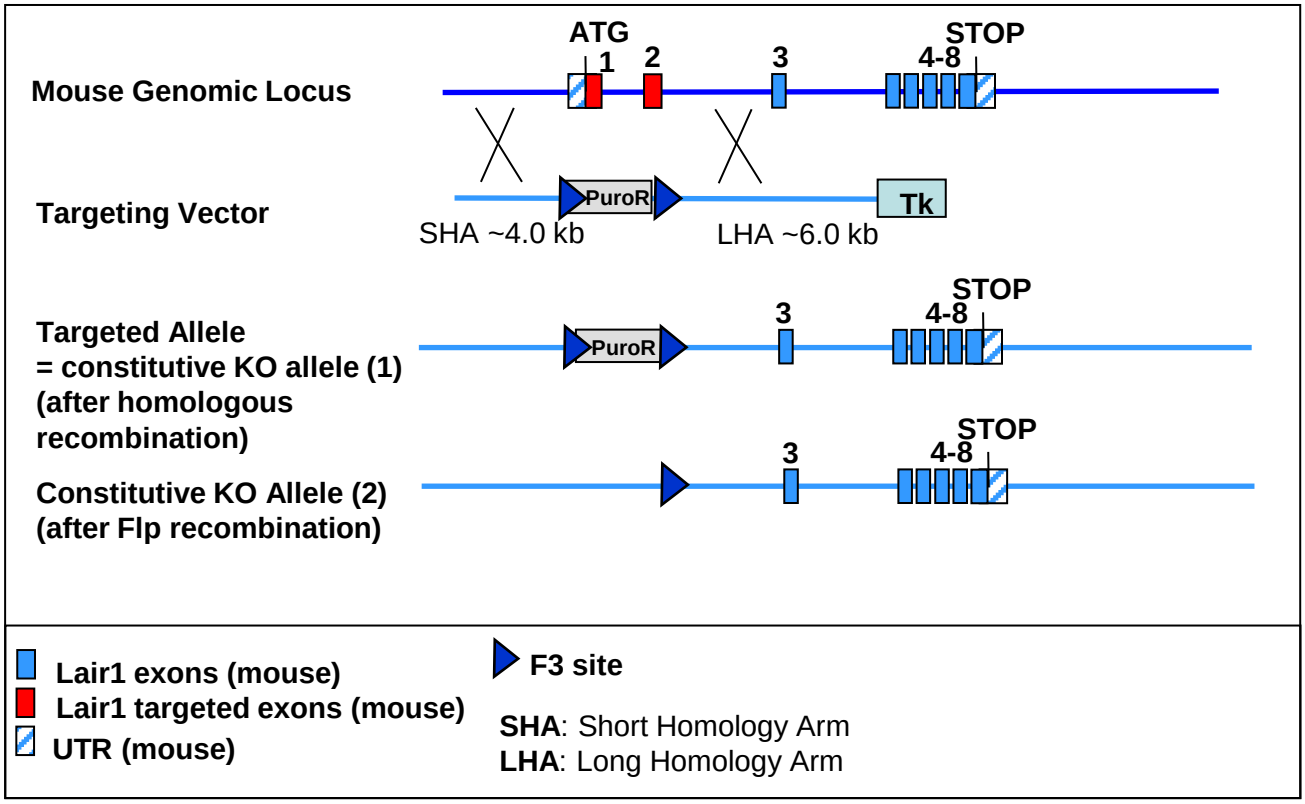

Supplemental Figure I. LAIR-1 targeting strategy.
Exons 1 and 2 have been replaced with a F3-flanked positive selection cassette (Puromycin resistance) expressed under the control of an eukaryotic promoter and containing a polyadenylation signal. Homologous recombinant clones will be isolated using positive (Puromycin resistance) and negative (Thymidine kinase - Tk) selection. The targeting vector has been generated using BAC clones from the C57BL/6J RPCIB-731 BAC library and will be transfected into the TaconicArtemis C57BL/6N Tac ES cell line. Replacing the proximal promoter and exons 1 and 2 with the positive selection cassette in the targeted allele (=constitutive KO allele) should result in the loss of function of the Lair1 gene by deleting the translation initiation codon and the sequence encoding the signal peptide. In addition, the deletion of the proximal promoter and the 5'UTR should prevent transcription of the Lair1 messenger RNA. Flp-mediated removal of the positive selection cassette also results in a constitutive KO allele. Heterozygous mice (-/+) were intercrossed to generate homozygous wild-type and mutant mice. The mice are viable, fertile, normal in size and do not display any gross physical or behavioural abnormalities.

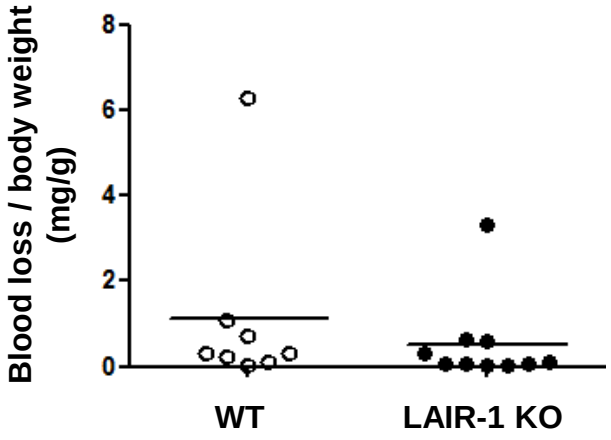

Supplemental Figure II. LAIR-1 KO mice do not exhibit a bleeding diathesis following tail injury. Normal blood loss of LAIR-1 KO (n = 10) mice compared with litter-matched wild-type (WT) mice (n = 9) in the tail bleeding assay (3 mm cut). Symbols represent individual mice. Horizontal line represents mean.

Supplemental Figure III

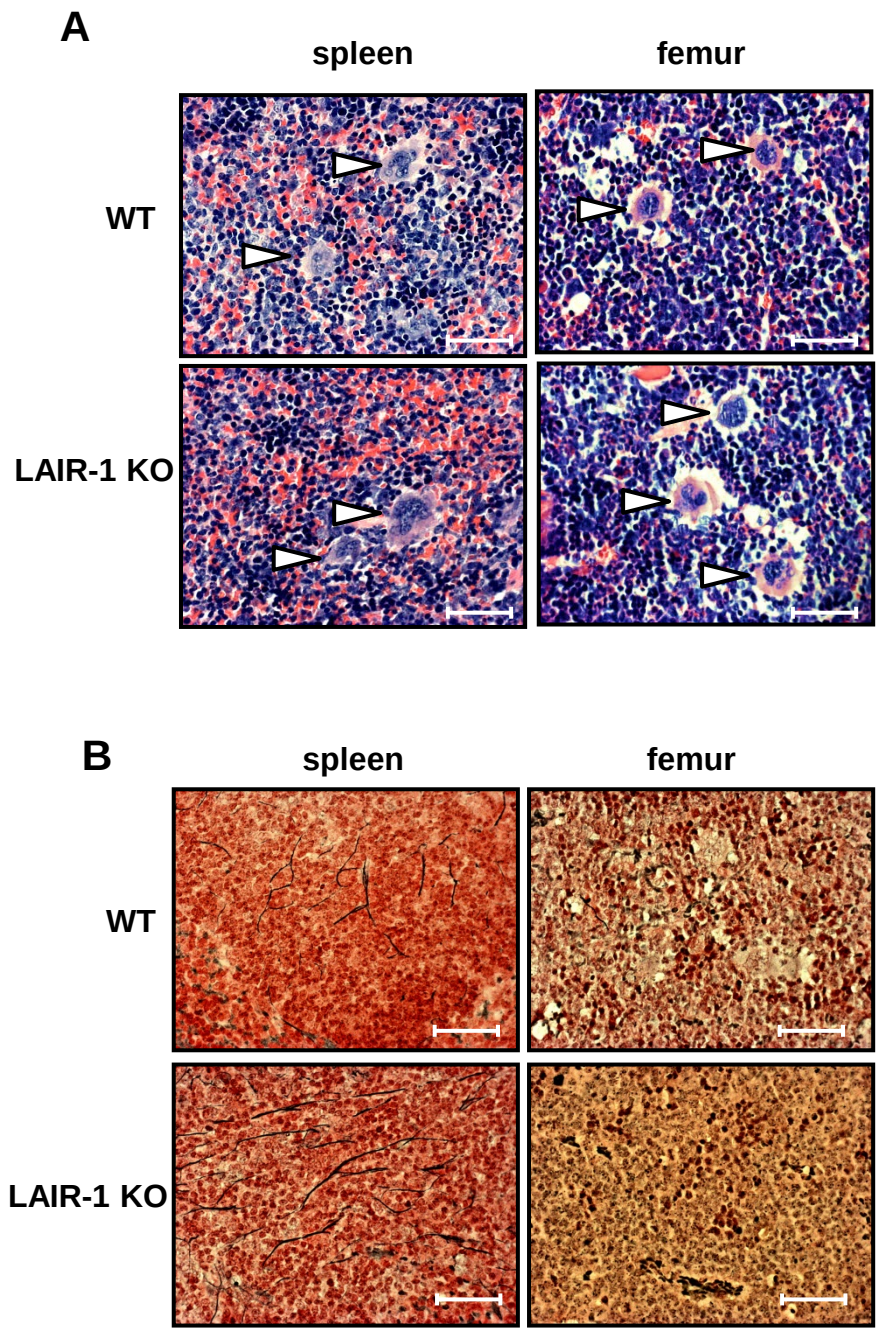

Supplemental Figure III. Normal haematopoiesis in LAIR-1 KO mice. **(A)** H&E- and **(B)** reticulin-stained spleen and femur sections from litter-matched WT and LAIR-1 KO mice. Representative images from n = 5 mice/genotype, 8-10 fields of view per tissue sample, through five marrow or spleen sections. Bright field images were obtained using a Zeiss Axiovert 200 inverted high-end microscope (Welwyn Garden City, UK) with a 20× objective. Arrowheads indicate megakaryocytes (scale bar = 50 μm). **(C)** Quantification of the number of megakaryocytes per field.

A

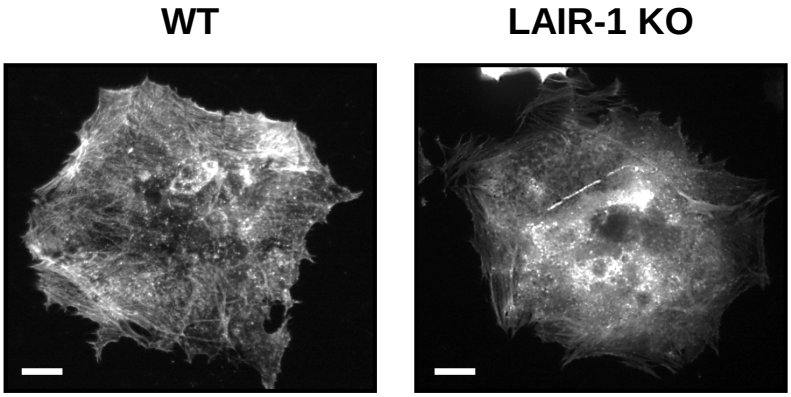

B

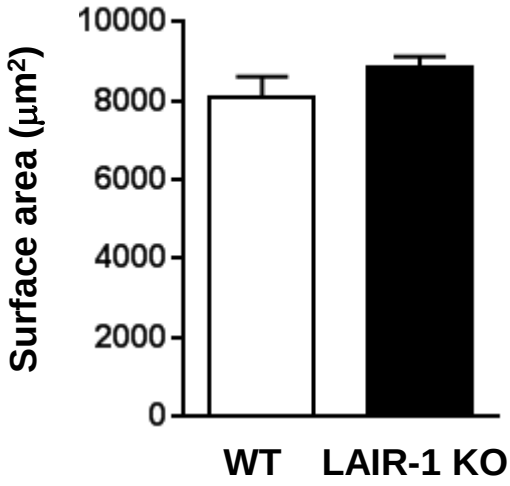

Supplemental Figure IV. Normal megakaryocyte spreading on collagen. (A) Bone marrow-derived megakaryocytes from litter-matched WT and LAIR-1 KO mice were plated on collagen-coated surface (100 μg/mL) for 5 hours at 37°C. Representative images of spread megakaryocytes (Alexa Fluor 488-phalloidin stained); scale bar represents 20 μm. **(B)** Megakaryocyte surface area was measured; n = 3/genotype, 20-50 megakaryocytes/genotype; mean ± SEM.

Supplemental Figure V

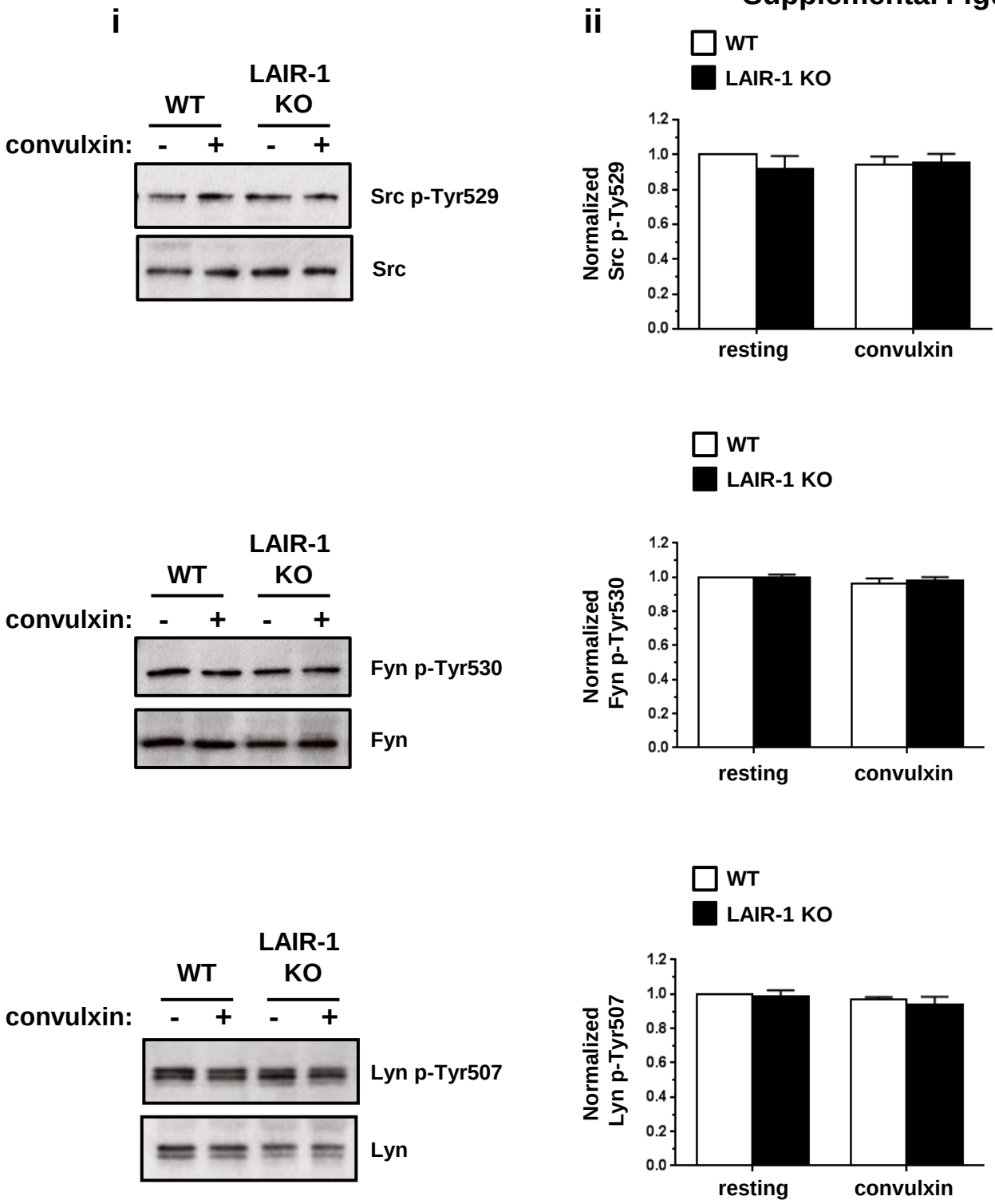

Supplemental Figure V. GPVI proximal signalling in LAIR-1 deficient megakaryocytes. Bone marrow-derived megakaryocytes from litter-matched WT and LAIR-1 KO mice were stimulated with 30 μg/mL convulxin for 15 minutes at 37°C. Whole cell lysates were western blotted with anti-Src p-Tyr529, anti-Fyn p-Tyr530 and anti-Lyn p-Tyr507 antibodies. Membranes were stripped and reblotted with anti-Src, anti-Fyn and anti- Lyn antibodies. **(i)** Representative blots and **(ii)** densitometry quantification from n = 3 independent experiments/genotype (mean ± SEM).

Supplemental Figure VI

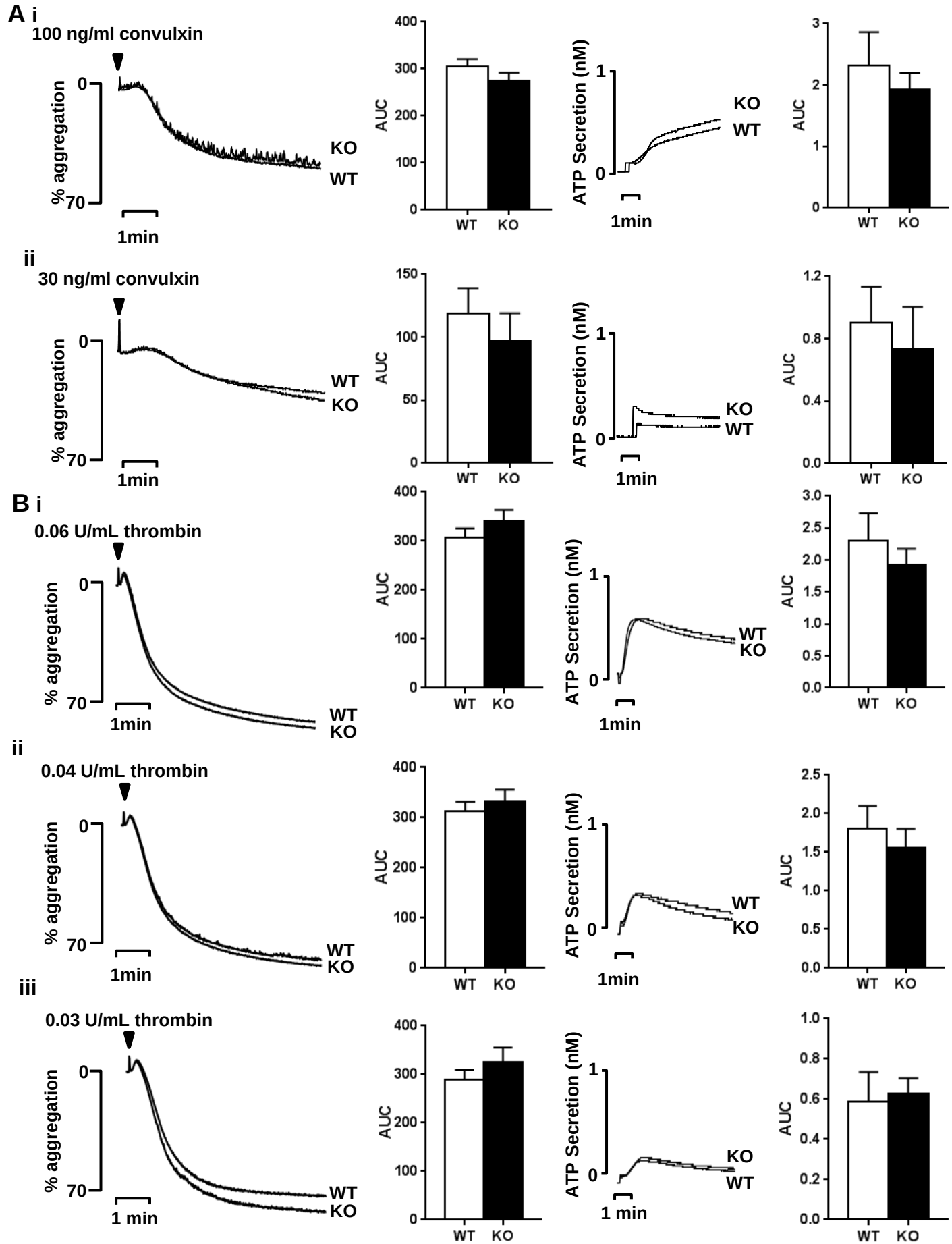

C

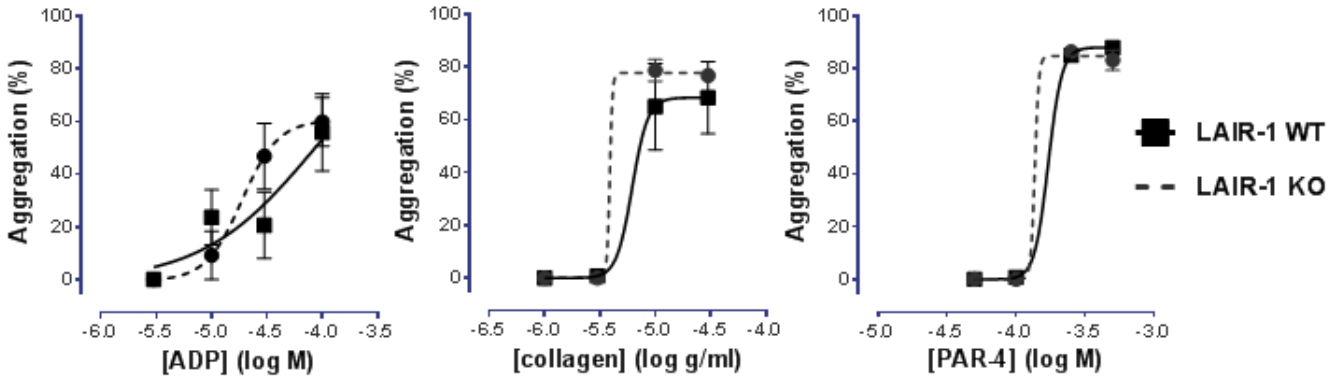

D

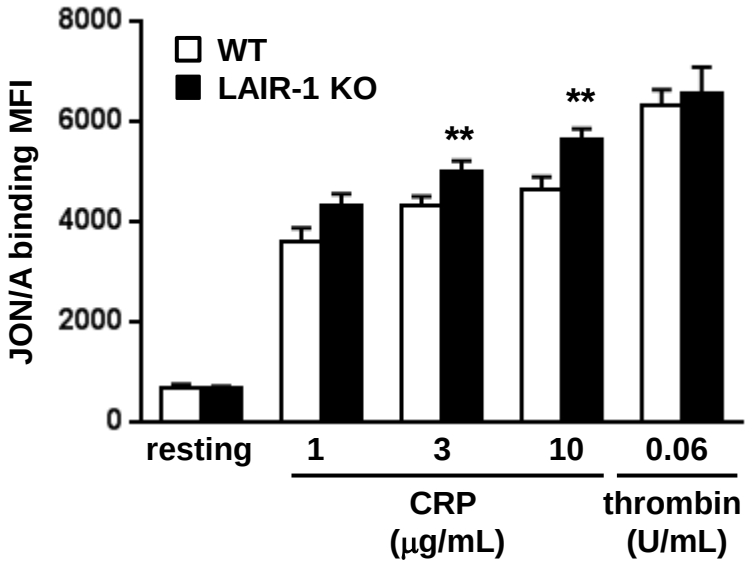

Supplemental Figure VI. Platelet reactivity in LAIR-1 KO mice. **(A)** Platelet aggregation and ATP secretion of washed platelets were measured by lumi-aggregometry in response to **(Ai-ii)** 30 and 100 ng/mL convulxin and **(Bi-iii)** 0.03, 0.04 and 0.06 U/mL thrombin. Representative traces are shown, n = 10-11 mice/genotype/condition. Quantification of time to area under the curve (AUC) of platelet aggregation and ATP secretion were measured. Mean ± SEM are represented. **(C)** 96-well microlitre plates (Greiner Bio-One, Stonehouse, Gloucestershire, UK) were precoated with hydrogenated gelatine (0.75% w/v) in PBS to block the surface activation of platelets before the addition of the platelet agonists. PRP or PPP was added into the appropriate control (agonist-free) and agonist-containing wells. The plate was sealed with film and then placed on a heater/shaker at 37ºC to mix at 1200 rpm for 5 minutes. Absorbance was then measured at 650 nm on a standard 96-well plate reader. Platelet aggregation was expressed as the maximal percent change in light transmittance from PRP wells in response to agonists, using PPP as reference, n = 3-4 mice/genotype/condition. **(D)** JON/A binding of platelets from litter-matched WT and LAIR-1 KO mice in response to 1, 3 and 10 μg/mL CRP and 0.06 U/mL thrombin were measured. Geometric mean fluorescence intensity (MFI) ± SEM is represented; n = 6 mice/genotype; ***P* < 0.01.

Supplemental Figure VII

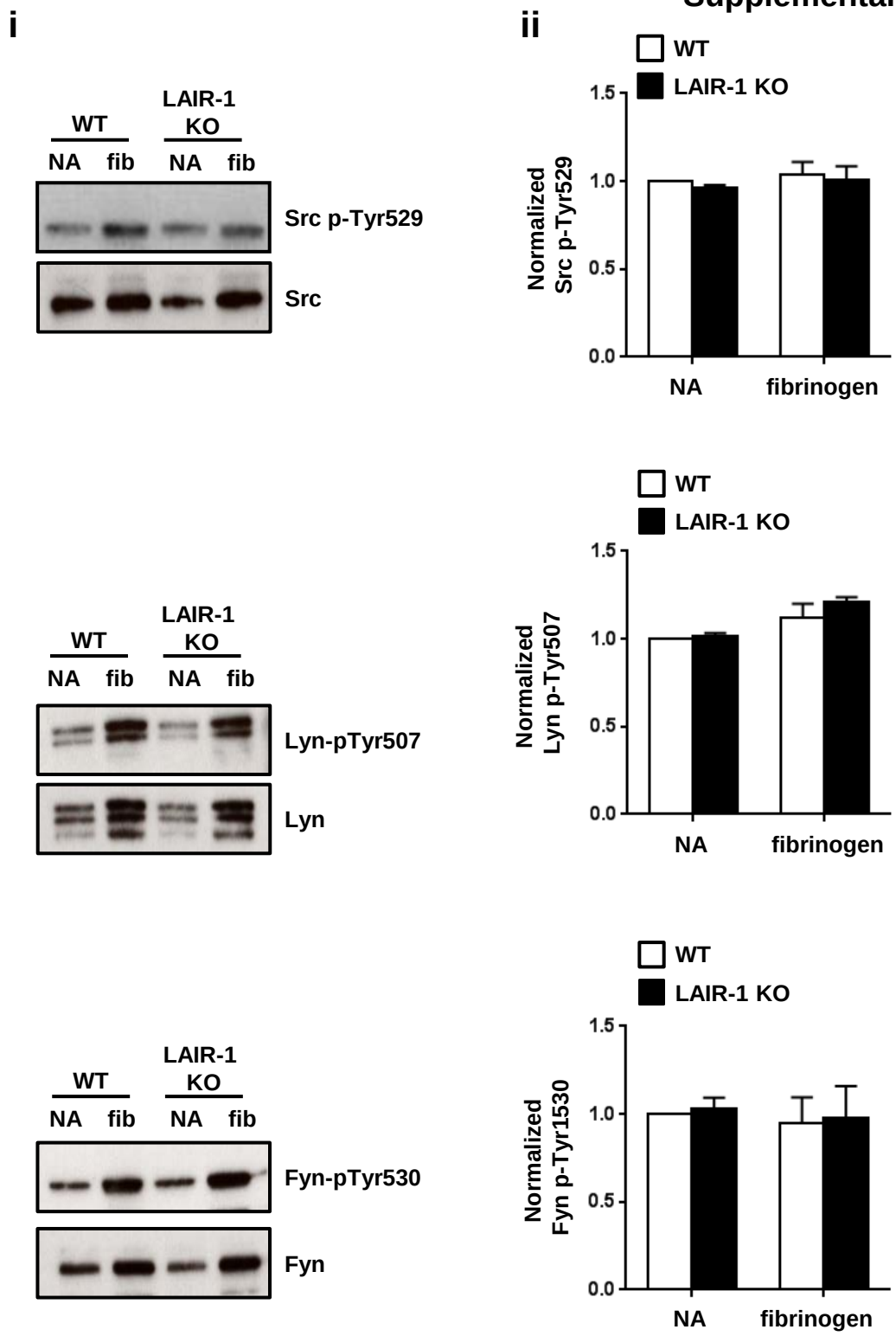

Supplemental Figure VII. Platelet αIIbβ3-integrin signalling in LAIR-1 KO mice. Washed platelets from litter-matched WT and LAIR-1 KO mice were plated on fibrinogen-coated surface for 45 minutes at 37ºC. Whole cell lysates were prepared from non-adherent (NA) and fibrinogen-adherent (fib) platelets and were western-blotted with anti-Src p-Tyr529, anti-Lyn p-Tyr507 and anti-Fyn p-Tyr530. Membranes were stripped and reblotted with anti-pan Src, anti-Lyn and anti-Fyn. **(i)** Representative blots and **(ii)** densitometry quantification from n = 3 independent experiments/genotype (mean ± SEM).

Supplemental Figure VIII

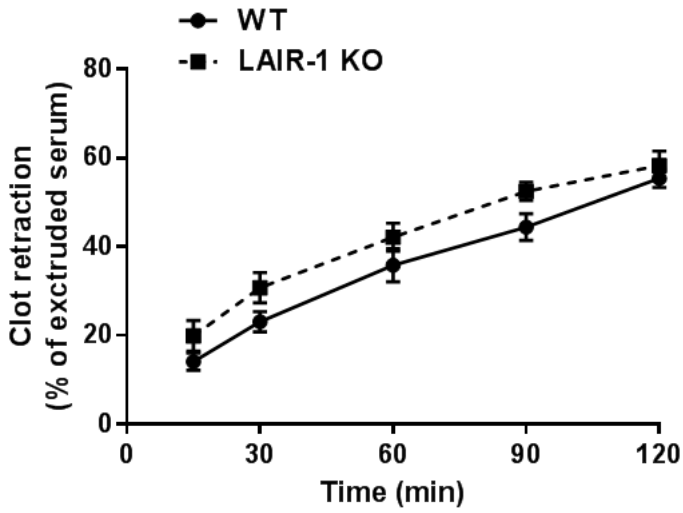

Supplemental Figure VIII. Normal clot retraction in LAIR-1 KO mice. Clot retraction of platelets in platelet rich plasma (PRP) from litter-matched WT (n = 10) and LAIR-1 KO mice (n = 8) upon activation with 10 U/mL thrombin in the presence of 2 mM $CaCl_2$ and 2 mg/mL fibrinogen. % of extruded serum over time is represented. Values are mean ± SEM.

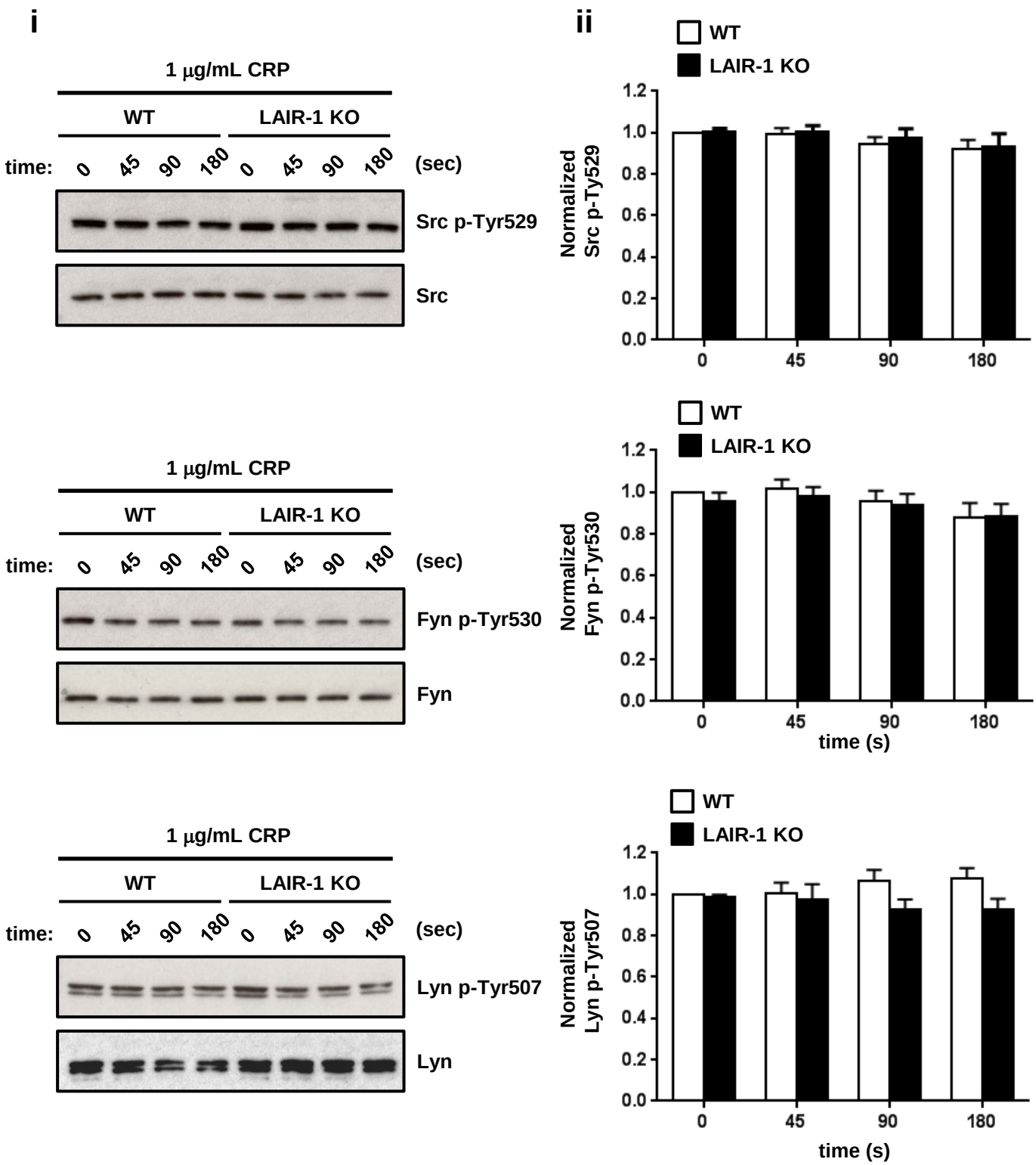
A
i
ii
1 μg/mL CRP
WT
LAIR-1 KO
time:
0
45
90
180
(sec)
Src p-Tyr529
Src
Fyn p-Tyr530
Fyn
Lyn p-Tyr507
Lyn
Normalized Src p-Ty529
Normalized Fyn p-Tyr530
Normalized Lyn p-Tyr507
time (s)

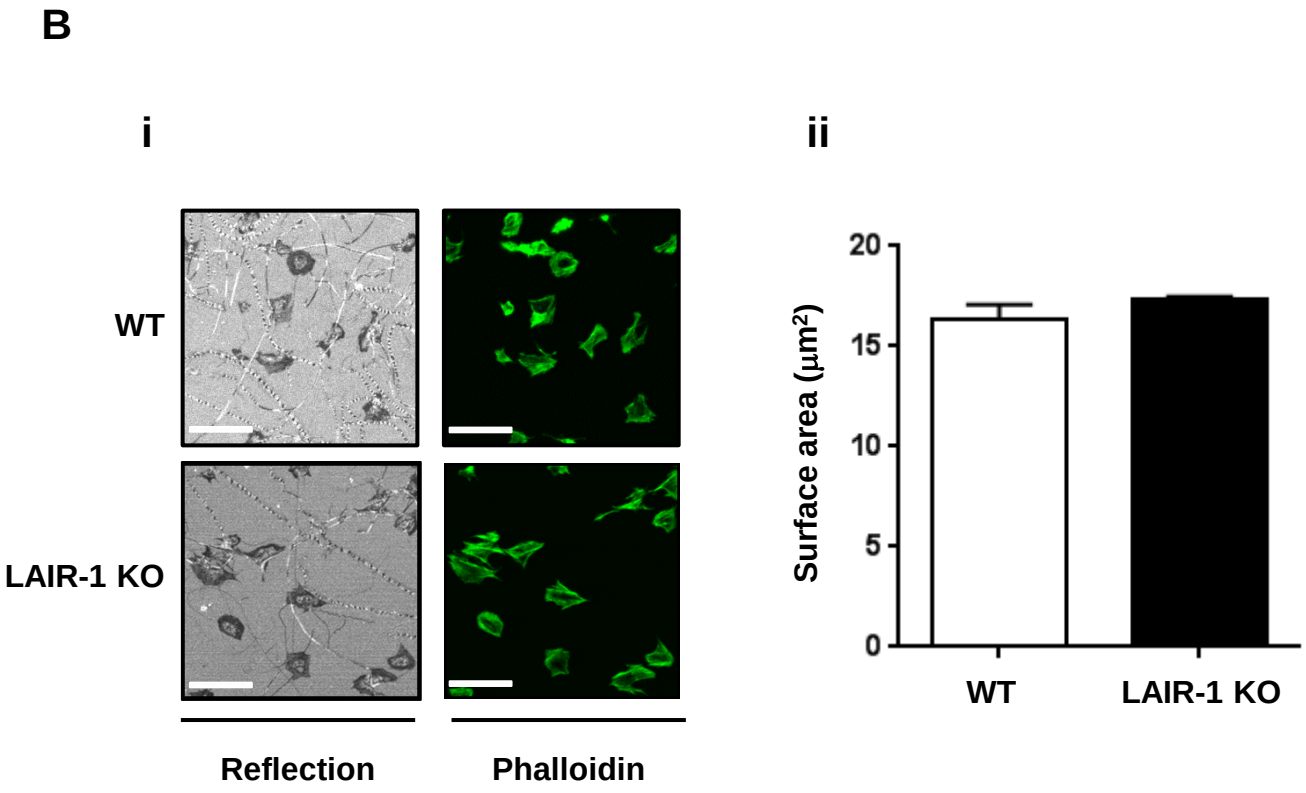

Supplemental Figure IX. GPVI proximal signalling in platelets from LAIR-1 KO mice. (A) Whole cell lysates of resting and 1 μg/mL collagen-related peptide (CRP)-stimulated platelets from litter-matched WT and LAIR-1 KO mice were western blotted with anti-Src p-Tyr529, anti-Fyn p-Tyr530 and anti-Lyn p-Tyr507 antibodies. Membranes were stripped and reblotted with anti-Src, pan Fyn and pan Lyn antibodies. **(Ai)** Representative blots and **(Aii)** densitometry quantification from n = 3 independent experiments/genotype (mean ± SEM). **(B)** Platelets from litter-matched WT and LAIR-1 KO mice were plated on collagen-coated surface (100 μg/mL) for 45 minutes at 37ºC. **(Bi)** Representative confocal reflection and phalloidin-stained images of platelets; scale bar: 10 μm. **(Bii)** Surface area of individual platelets in confocal reflection images was measured; n = 5/genotype, 140-220 platelets/genotype; mean ± SEM.

Supplemental Videos

Supplemental Video I (for Figure 7D). Laser-induced thrombus formation in an arteriole of a WT mouse. WT mice were injected with DyLight488-conjugated anti-GPIbβ antibody (X488) via the carotid artery. Fluorescently-labelled platelets (green) are shown accumulating at the site of a laser-induced injury in an arteriole of the cremaster muscle. A timer is show in the top left corner and a 10 μm scale bar in the bottom left corner. Representative video of twenty-three thrombi induced in 4 WT mice.

Supplemental Video II (for Figure 7D). Laser-induced thrombus formation in an arteriole of a LAIR-1 KO mouse. LAIR-1 KO mice were injected with DyLight488-conjugated anti-GPIbβ antibody (X488) via the carotid artery. Fluorescently-labelled platelets (green) are shown accumulating at the site of a laser-induced injury in an arteriole of the cremaster muscle. A timer is show in the top left corner and a 10 μm scale bar in the bottom left corner. Representative video of seventy-three thrombi induced in 12 KO mice.

Supplemental Video III (for Figure 7E). Ferric chloride-induced thrombus formation in the carotid artery of a WT mouse. WT mice were injected with DyLight488-conjugated anti-GPIbβ antibody (X488) via the jugular vein. Exposed carotid arteries from WT mice were injured with 10% ferric chloride for 3 minutes. Fluorescently-labelled platelets (green) are shown accumulating at the site of an injury over 15 minutes. A timer is shown in the top left corner and a 200 μm scale bar in the bottom left corner. Representative video of thrombus formation from 10 WT mice.

Supplemental Video IV (for Figure 7E). Ferric chloride-induced thrombus formation in the carotid artery of a LAIR-1 KO mouse. LAIR-1 KO mice were injected with DyLight488-conjugated anti-GPIbβ antibody (X488) via the jugular vein. Exposed carotid arteries from LAIR-1 KO mice were injured with 10% ferric chloride for 3 minutes. Fluorescently-labelled platelets (green) are shown accumulating at the site of an injury over 15 minutes. A timer is shown in the top left corner and a 200 μm scale bar in the bottom left corner. Representative video of thrombus formation from 10 LAIR-1 KO mice.

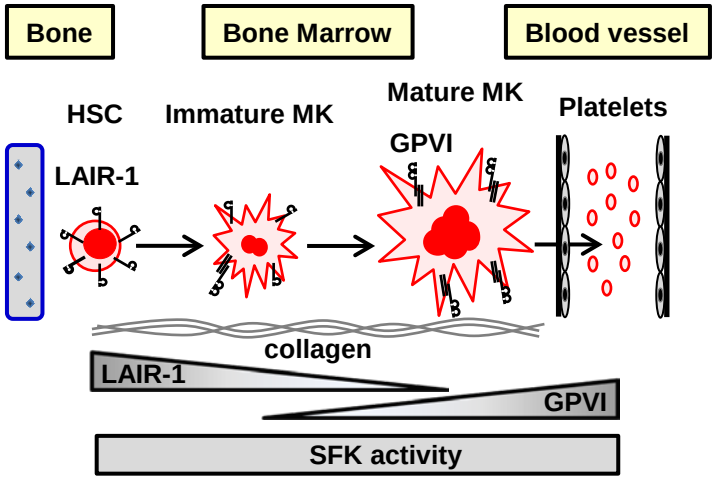

Wild-type

- LAIR-1 is expressed in haematopoietic stem cells (HSCs)
- LAIR-1 is downregulated during megakaryocyte (MK) development
- GPVI-FcRγ chain complex is upregulated during MK development
- Low basal Src Family Kinase (SFK) activity in MKs and platelets

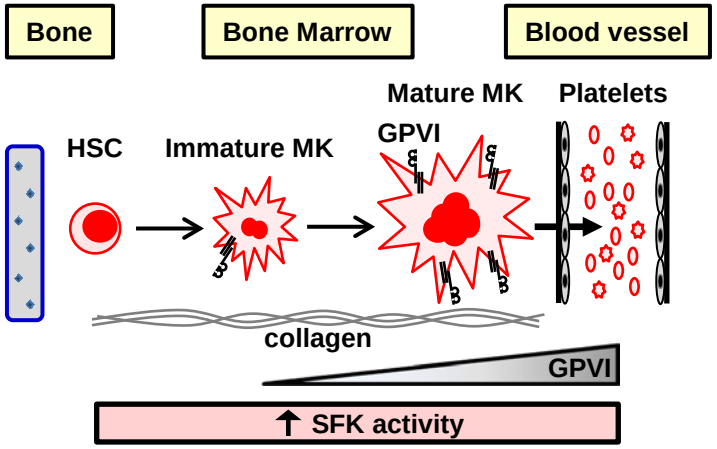

LAIR-1 KO

- Increased platelet count and life-span
- Platelets hyper-reactive to collagen
- Increased $FeCl_3$-induced thrombus formation in the carotid artery
- Increased SFK activity